CSIRO Marine Laboratories
Report 226

# Remote Sensing of Algal Blooms in the Swan River

## CSIRO Blue-Green Algal Multi-Divisional Program

**P. Jernakoff[1], P. Hick[2], C. Ong[2], W. Hosja[3], S. Grigo[3]**

[1] CSIRO Division of Fisheries
[2] CSIRO Remote Sensing Unit, Division of Exploration and Mining
[3] Waters and Rivers Commission

CSIRO
AUSTRALIA
**March 1996**

CSIRO Marine Laboratories
Report 226

# Remote Sensing of Algal Blooms in the Swan River

## CSIRO Blue-green Algal Multi-Divisional Program

**P. Jernakoff**
**P. Hick**
**C. Ong**
**W. Hosja**
**S. Grigo**

CSIRO Division of Fisheries
Marine Laboratories
Castray Esplanade
GPO Box 1538, Hobart, Tasmania 7001

**National Library of Australia Cataloguing-in-Publication**

Remote sensing of algal blooms in the Swan River: CSIRO Blue-Green Algal Multi-Divisional Program

Includes index
ISBN 0 643 05792 7.

1. Cyanobacterial blooms - Western Australia - Swan River - Remote sensing. 2. Cyanobacteria- Western Australia - Swan River - Remote sensing. I. Jernakoff, Peter. II. CSIRO. Marine Laboratories. III. CSIRO. Division of Fisheries. (Series : Report (CSIRO. Marine Laboratories) ; 226).

589.56099412

# Summary

This study was part of a larger project by the CSIRO Multi-Divisional Blue-Green Algal Program: "Automatic remote monitoring of water quality and remote sensing of algal and cyanobacterial blooms in Australian inland and estuarine waterways". The remote sensing component was seen as important because there is a need for cost-effective techniques to detect algal blooms over large areas and to monitor, in near-real-time, the widely distributed water bodies in Australia.

While most algae problems in the eastern states of Australia are caused by cyanobacteria, the Swan River in Western Australia experiences phytoplankton blooms of green algae, diatoms and dinoflagellates. The ability to spectrally discriminate between types of blooms was a major objective of the study.

The use of airborne instruments was also evaluated as a low-cost, operational supplement to traditional boat-based sampling for assessing the spatial and temporal extent of algal blooms. Field studies of in-water reflectance, using multi-band radiometers, were supported by laboratory studies that indicated that significant spectral differences between cyanobacterial and green algae and diatoms/dinoflagellates were measurable.

Two types of airborne multispectral spectral instruments were evaluated:

(1) the CASI (Compact Airborne Spectrographic Imager), which has 288 bands in imaging-spectrometer mode and 14 bands in spatial-imaging mode. It therefore has high spectral resolution, but has the disadvantage of producing very large data sets that require significant time to process and analyse. The system was also not available at short notice ; and

(2) the DMSV (Digital Multi-Spectral Video) provided less spectral resolution, although the bands could theoretically be selected to provide maximum discrimination of algal blooms. The DMSV was less expensive to operate and was normally available at short notice.

Because of the logistical constraints in measuring sufficient numbers of replicates of in-water spectra during over-flights by airborne scanners, the study examined the implications of bloom stability (in space and time) and the time and duration of airborne data collection compared with and the data collected from ground surveys.

Our research into remote sensing with an airborne system of the Swan River and surrounding waterways, identified some advantages and limitations to the generic use of this technology. These are illustrated in the following points and the supporting images.

• Remote sensing is an effective means of rapidly mapping the extent of highly dynamic, widely spread algal blooms. Airborne sensors have advantage the over traditional sampling methods that they can sample large expanses relatively cheaply and quickly. *Remote sensing provides a "bird's-eye view" of blooms and is a unique means of identifying specific sites of interest such as inflowing drains and "hot-spot" sites, which may be difficult to identify or locate from the ground.*

• Most discrimination of algal bloom types can be made with few a spectral bands in the visible spectrum, which will cover the main combinations of pigments. *For routine monitoring, simple instruments such as the DMSV should be sufficient, provided that bandpass filters are selected for maximum discrimination of the bloom of interest from the water column.*

• More research on the spectral contribution of water-column components (e.g. humics, suspended solids) will provide a more quantitative description of bloom type and severity when specific algorithms for image analysis are developed.

Several factors can result in artefacts within the DMSV images, which limit the usefulness of data and hence the ability to interpret the extent and severity of a bloom accurately. Some of these can be minimised by careful flight planning and adopting the following protocol:

• Flight times should coincide with sun angles of < 45 degrees (which usually means that in summer, flights should be between 8am and 10am, and between 3pm and 5pm. *Some algal blooms (e.g.* Gymnodinium) *change their position in the water column so that their maximum abundance in the surface layers occurs in the latter part of the day. Thus flights need to be planned to coincide with both physical and biological factors for maximum accuracy.*

• A 50% overlap of the DMSV image frames will also minimise the effects of sunglint. Optimum data quality is obtained when calm wind conditions prevail, because the smaller wave ripples minimise sunglint and the upper water column is not being mixed by wind. The central flight-line for the aircraft can also be set to favour the same side of the river as the sun to minimise sunglint effects.

• Flight altitudes of 3,500 m provide DMSV images with 2 m pixels (nominal ground resolution), which gives excellent spatial discrimination.

• Calibration targets should be included in every mission, and gains and offsets of cameras should not be altered without reflight over those targets.

• Camera alignment on the DMSV should be precise to ensure a minimum of post-processing registration of 1.5 m to 2 m pixels; individual frames can be easily mosaiced if overlayed on 10 m pixel satellite data such as panchromatic SPOT.

• Further development of automatic correlation-based software procedures to process data for near-real-time information products is essential. *Using the procedures developed for this study, the delivery time for image products is around of two to three days; this could be reduced to less than 24 hours.*

• Ground-truthing must be done within ± 30 min of flight times, or bloom distribution and abundance may have significantly changed and have little resemblance to the patterns captured in the image. *A way to ensure better-ground truthing at the time of the overflight is to deploy multiple fluorometers from stations or boats equipped with differential GPS.*

• The recent development of miniature field spectrometers should be pursued. These instruments have the potential to supplement the use of fluorometers and also be useful for remote monitoring and identification of algal types based on characteristic spectra, as well as for validating airborne imagery.

# Contents

**Figures**



**Tables**

# Background

Concern over algal blooms in inland and estuarine waterways is growing in Australia (Hosja 1992); as well as many other parts of the world (Smayda, 1990). Both the frequency and spatial extent of blooms have increased, largely through nutrients flowing into the waterways from treated sewage, plant fertilisers and detergents (Hallegraeff, 1993).

Some algal bloom species are extremely toxic to humans and animals, others cause skin irritations; and others, by their sheer weight of numbers, use up oxygen when they die, which results in fish kills and lower water quality (Anderson, 1989).

While most blooms in the rivers and wetlands of the eastern states of Australia are caused by cyanobacteria, the main study site in the Swan River in Western Australia, experiences green, diatom and dinoflagellate algae blooms. Other river systems in Western Australia, e.g. the Canning River, also experience cyanobacteria blooms (Hosja and Deeley, 1994).

In response to algal bloom problems increasing nationally, CSIRO allocated priority funds in 1992 to support research into the cause and nature of blooms, ways to reduce their frequency, intensity and impact, and methods to identify toxic strains. They also funded methods of remotely monitoring blooms, including remote sensing to examine spatial and temporal scales of variability, which is not readily possible with traditional phytoplankton sampling strategies.

The present study, "Remote sensing of algal blooms in the Swan River" is part of a larger project: "Automatic remote monitoring of water quality and remote sensing of algal and cyanobacterial blooms in Australian inland and estuarine waterways". This project was undertaken because there is a need for cost-effective techniques to detect algal blooms over large areas and to monitor, in near real-time, the widely distributed water bodies in Australia.

Studies on remote sensing of algal blooms usually use data from satellite or airborne systems. Both types of platforms use multispectral band combinations that detect reflected radiation within the visible and near-infrared parts of the electromagnetic energy spectrum. Spectral characteristics of particular water bodies, and more importantly, of particular pigments within algal bloom cells means that it is theoretically possible to reliably detect these pigments.

Satellite data have been used to map algal blooms and water quality. Carpenter and Carpenter (1983); Lillesand et al. (1983); Verdin (1985); Dwivedi and Narain (1987) all showed the value of remotely sensed data for measuring water quality. In Western Australia, Pattiaratchi et al. (1990), Lavery et al. (1992), and Lavery et al. (1993) have shown the potential for the routine use of satellite-derived data for quantitatively measuring chlorophyll concentrations in Cockburn Sound and Peel Inlet. However, those studies also showed that it was impossible, with current satellite systems, to differentiate species by chlorophyll pigments. In addition, cloud cover at satellite overpass times in the Perth area means there is about a 40% probability of clear acquisitions.

Airborne systems have several advantages over satellites. These include the ability to schedule flights to coincide with optimal weather or bloom conditions; to focus on particular dynamic regions; and to choose spatial and spectral resolutions (Zibordi et al., 1990; Harrison & Jupp, 1990). However, there are also disadvantages, such as brightness variation in the geometrical scene; platform instability and navigation errors make it difficult to mosaic images between flight lines; and the area covered during flight is generally smaller than that from satellites, so full coverage is generally more expensive (Harrison & Jupp, 1990). Even so, airborne systems are usually

much less expensive than traditional boat-based sampling to cover similar-sized areas.

The aim of the present study was to evaluate the use of airborne remote sensing as an operational tool for mapping algal blooms types in the Swan River. In-water spectra were collected with a variety of instruments to measure algal spectra in the river for baseline data, to verify that algal bloom types could be distinguished (e.g. green algal blooms from dinoflagellates), and to assist in discriminating blooms by remote sensing techniques.

Two types of airborne systems were used, so the report is in two parts to reflect the sequence in which they were used. The two systems the Compact Airborne Spectrographic Imager (CASI) and the Digital Multispectral Video (DMSV). The use of these systems was based on their availability. CASI was brought to Australia by COSSA in the summer of 1993-4 before the study officially began.

# The Study Area

The Swan River flows through Perth, the capital city of Western Australia, and joins the sea at Fremantle. It has a catchment of 124 000 sq km, of which about 70% has been cleared for dryland agriculture, with the remaining area being native eucalypt forest. A large proportion of the metropolitan area and the near-urban intensive farms drains into the estuaries of the Swan/Canning system, around which live about one million people (Figure 1).

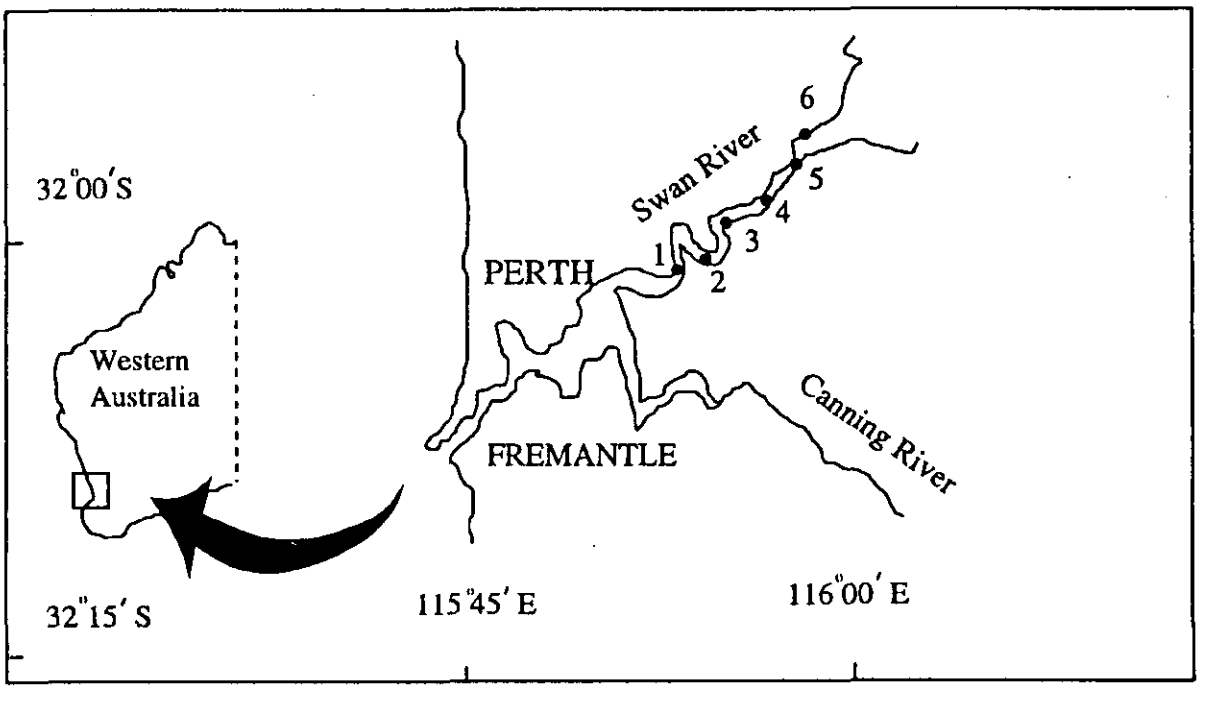


**Figure 1: Map of the study area, showing the six monitoring sites in the upper reaches of the Swan River**

The input of nutrients (principally agriculture-derived phosphate and nitrate from the predominantly winter rainfall and humic-rich groundwater) to the river has resulted in frequent algal blooms of increasing intensity and toxic severity. The distribution of phytoplankton in the Swan River estuary is controlled by dynamic environmental factors, but the phytoplankton is predominantly composed of diatoms and phytoflagellates (John, 1987). Diatom blooms occur during the winter in the lower estuary and throughout the estuary in summer and autumn, while massive phytoflagellate blooms appear in the spring. An incursion of clear marine saline water progresses up the river system during the summer, replacing the humic-rich, less saline, winter river flow.

# Baseline Spectral data

Laboratory studies of bloom types and mixtures have shown the additive nature of the spectral response of phytoplankton and the diagnostic potential of spectral signatures for determining those blooms (Johnsen et al., 1994). Field measurements of algal spectra were made to determine whether algal groups (green algae, diatoms, dinoflagellates) could be distinguished on the basis of their spectral characteristics within the matrix of other water constituents such as humics and sediments; and then to determine whether the water-leaving radiance could be reliably measured by an airborne sensor.

# Fundamentals of in-water spectral measurement

The approach to be taken for the measurement of above- and in-water spectra is determined on the basis of the following: the basic models for the measured energy recorded at an airborne sensor (i.e. the radiance, R), at waveband, w, may be resolved into components involving the atmosphere and radiation leaving the water surface such that:

$$R = tw(Lw + Lsw) + Law \qquad (1)$$

where:

R is radiance recorded at the sensor,
w is the waveband
tw is total atmospheric transmittance,
Lw is radiance from the water column,
Lsw is radiance reflected from the water surface, and
Law is radiance scattered into the sensor field of view by the atmosphere, or sky, radiance.

The above-water measurement of radiation emerging from the water column (Lw) includes effects of depth, bottom type and particulates in the water column, as well as the reflected component (Lsw). When sun angles produce "sun glint" or "ripple-flaring", (Lw) and (Lsw) may need to be corrected.

(Lw) has constituent components that need further consideration. These may be suspended solids such as sediments, dissolved substances or chlorophyll-based material in the water column, or the textural components of the bottom. (Lw) is measured either against a Lambertian standard or against a measure of irradiance (tw + Law = tmw) from the upward-pointing diffuser. (Lsw) can then be derived, in a crude form, by measuring with the radiometer above and below the water's surface skin. This may be modelled as follows:

$$Lw = tmw\ Lbw + (1-tmw)Lmw \qquad (2)$$

where:

Lw is the measurable radiance from the water column
tmw is the effective transmittance
Lbw is the radiance from the substrate material
Lmw is the radiance of the water column materials

As (tmw) varies between 0 and 1, (Lw) varies between (Lmw) and (Lbw) (i.e. deep water to no water cover at all or, in the case in the Swan River to date, where Lbw and Lmw are low or zero). Therefore, measurements made in the Swan River are designed to provide three factors:

1. total water-leaving radiance
2. radiance from the surface
3. radiance from the column, on the assumption that there is no radiance from the bottom.

# DSIR and Irricrop radiometers

Field measurements were made with radiometers, borrowed when available. The DSIR radiometer, manufactured by DSIR (New Zealand), was enclosed in an underwater housing and suspended from a frame that allowed the vertical alignment of the meter to be reversed so that the sensors could face either downwards or upwards. Nominal centre wavelengths are shown in Table 1. The ratio of upwelling to downwelling light was used to calculate a percent reflectance for each of the spectral bands. The second radiometer, the Irricrop, uses a simultaneous combination of eight upward and eight downward detectors with nominal band-centres, also shown in Table 1.

The underwater housings protected the radiometers and also ensured that the instruments remained stable in the water column, pointing directly upward or downward. The radiometers were connected by a waterproof cable to a laptop computer on a boat. Readings were made under full sun with a sun angle generally < 45° (cloudless skies and away from any shade generated by the boat).

Laboratory measurements of algal spectra to determine which bloom types were identifiable was curtailed because Johnsen et al. (1994) published the measurements we required. The results from our field and aircraft measurements also indicated that our effort would be effectively allocated to measuring spatial and temporal dynamics of the phytoplankton blooms and the relationship of *in situ* measurements to image classification.

***Table 1*** **The wavelength (in nanometres) of spectral bands for the DSIR and Irricrop field radiometers and the CASI and DMSV airborne scanners**

| No. | CASI | DMSV | Irricrop | DSIR | Purpose of CASI bands |
|---|---|---|---|---|---|
| 1 | 446-453 | 438-462 | 450 | 440 | Water penetration |
| 2 | 477-484 | | | 480 | Chlorophyll *a* |
| 3 | 497-504 | | 500 | | Ocean Chlorophyll *a* Ref. |
| 4 | 527-534 | | | 520 | Scattering |
| 5 | 547-554 | 538-562 | 550 | | Green Reference |
| | | | | 560 | |
| 6 | 564-572 | | | | Phycoerytherin pigment |
| 7 | 597-604 | | 600 | | Yellow Reference |
| 8 | 622-629 | | | 620 | Phycocyanin pigment |
| 9 | 647-654 | 638-662 | 650 | | Red Reference |
| 10 | 674-683 | | | 670 | Chlorophyll *a* pigment |
| 11 | 708-715 | | 700 | | Red edge Reference 1 |
| 12 | 746-755 | | 750 | | Red edge Reference 2 |
| | | 758-782 | | 780 | |
| 13 | 800-808 | | 800 | | Near-infrared Reference 1 |
| 14 | 844-851 | | | 860 | Near-infrared Reference 2 |

## Spectral Comparisons

Spectral measurements of algal blooms were made, initially with the DSIR and subsequently with the Irricrop radiometer, of a range of sites in the summers of 1992/3 and 1993/4. These measurements were made, where possible, simultaneously with aircraft missions and with biological, physical and chemical sampling.

Figure 2 (A), (B) and (C) is an example of 10 replicates of "in-water" spectral measurements (the ratios of the downward/upward) at the Ron Courtney Island site on 15 March 1994. The top graph (A) was measured with the radiometer suspended 1 metre above the water surface (Lw) but does not take account of atmospheric

radiance (Law) that would be scattered into the path of an airborne sensor. The middle graph (B) was measured with the downward (radiance) sensors of the radiometer just beneath the surface of the water and the diffuse upward (irradiance) sensors above the water surface. This provides an estimate of the surface reflectance (Lw - Lsw) or the combined contribution of column materials and substrate (Lmw+Lbw) and, as mentioned earlier, we assume no contribution from the bottom (confirmed by Secchi and light extinction measurements) and is basically the spectra of dissolved and suspended material in the water column.

In an attempt to separate between column components a third set of readings was made with the radiometer set at different depths below the surface. The lower graph (C) is in effect a ratio of the transmission through 25 cm of water between the surface and the upward diffuse sensors and the radiance from the deeper water. This was an attempt to quantify the proportions of "forward-scatter" and "back-scatter" by particles in the column. In most cases these values cancelled each other out in depths beyond 50-100 cm (usual Secchi extinction depths for the Swan River).

The points of note in these spectra are the removal of the surface scattered (blue-end) effects of the atmosphere between graphs (A) and (B). Also note the absolute reflectance values and the declining but consistent band-relationships throughout, even in graph (C), which shows more variability.

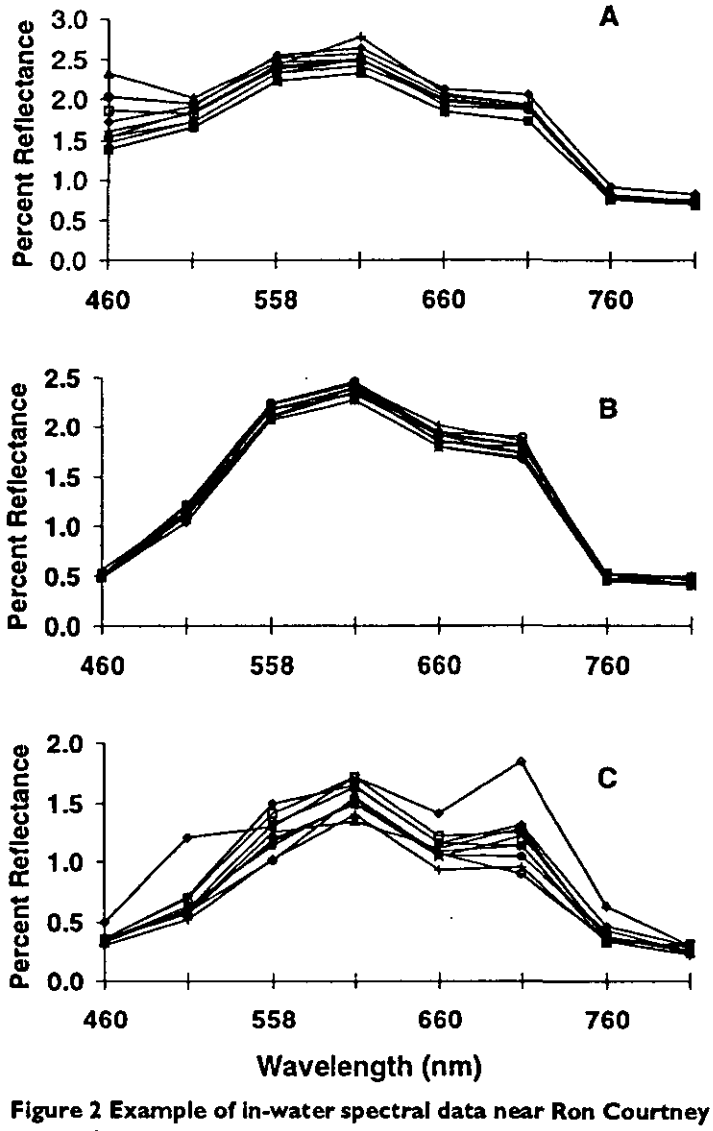


**Figure 2 Example of in-water spectral data near Ron Courtney Island In-water spectral measurements, recorded with the Irricrop radiometer, on 15 March 1994.**

It was thus possible to compare the spectral contributions of specific column constituents; Figure 3 is such a comparison of three bloom types that appeared in the Swan River system during the summer of 1993/4. The cyanobacteria (*Anabaena* sp.) bloomed near the Canning Weir and the green (*Chlamydomonas* sp.) was measured during an extensive bloom in the Bassendean area of the Swan River. The dinoflagellate (*Gymnodinium* sp.) bloomed in the Ascott area. The spectral differences in these bloom types are significant. On the basis of this analysis, a range of narrow band-pass spectral filters within 480-700 nm were planned for use in the airborne video system in an attempt to translate the "in-water" results to airborne imagery.

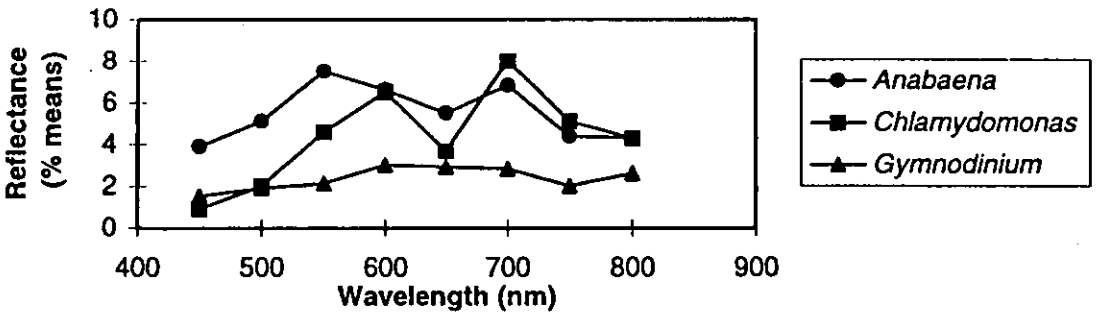


**Figure 3 An example of in-water spectral measurements showing spectra for cyanobacterial, green and dinoflagellate algal groups recorded in the 1992/3 summer in the Swan River system.**

# Ocean Optics Miniature Field Spectrometer

Recent developments in miniature fibre-optic spectrometers (made by Ocean Optics, Dunedin, Florida, USA) suggest that they may have the potential to identify bloom types in the field based on characteristic spectra. These solid-state instruments measure high-resolution spectra (1024 wavelengths) by holographic diffraction gratings in the reflected Ultra Violet, Visible and Near Infrared.

A prototype instrument was coupled directly to a portable computer to display and record both target and reference spectra. A range of optical fibre diameters and collecting optics were developed to provide the opportunity to resolve either absorption or reflectance spectra to 2 nm from a narrow or diffuse field-of-view.

This instrument was developed for laboratory or workbench applications by its manufacturers, but the ease with which it could be adapted for moored or boat applications suggests that it may have much potential as a future monitoring tool. The simplicity of connecting the optical fibre to any optical device and simultaneously measure incoming or sourced energy and target radiance made this instrument invaluable for real-time optical water-quality research; bloom type detection and concentration; and, monitoring and management strategies.

Spectral data from the Ocean Optics instrument are used to show concentrations of the algae Gymn*odinium simplex* later in this report (see Figure 16).

# CASI Related Studies

The Compact Airborne Spectrographic Imager (CASI) was flown over parts of the Swan River to evaluate remote sensing for detecting and monitoring algal blooms. It was flown in both spectral (288 bands x 39 lines) and spatial (14 bands x 512 lines) modes to address four generic objectives. These were:

- to compare the controlled in-water **field spectral** measurements, taken with submerged radiometers, with the high-resolution CASI **spectral-mode** measurements, taken from the aircraft
- to compare the **biological** measurements with the high-resolution CASI **spectral-mode** measurements in order to determine possible diagnostic wavebands
- to compare the **physical** and **biological** measurements with **spatial-mode** CASI data in order to test the selection of aggregated bands
- to simulate the data produced from low-cost, video-based systems for this type of work

The limited availability of CASI meant that it was not flown during a major bloom event in the Swan River. However, there was a reasonable range (5000-31000 cells/mL) of concentrations and, in wetlands associated with the river, significant cyanobacterial and green algal blooms. The wetland sites were not sampled simultaneously with the over-flight, but subsequent inspection and anecdotal evidence confirmed the presence of these bloom types (probably *Anabaena sp.* at above 100 000 cells/mL; *pers. comm.* W. Hosja, Water and Rivers Commission).

# Methods

## CASI

The CASI (Compact Airborne Spectrographic Imager) is based on an f/4 reflection grating spectrograph coupled to a CCD array of 578 spatial pixels dispersed over 288 bands, (Babey and Anger, 1989). To handle the high data rates, the CASI can be flown in one of two modes: in **spatial-mode,** up to 15 full-image bands between 423 and 946 nm can be acquired across a field of view of 35°; in **spectral-mode**, 288 contiguous bands of 39 evenly spaced picture elements or "rakes" chosen within the same field of view can be acquired. The flight lines need to be flown twice to capture data in both modes.

The CASI instrument was brought to Western Australia for evaluation in February 1993 and installed in a Britten-Norman Islander aircraft. A gyroscope to record aircraft roll, a GPS and a drift-site for site location were also fitted.

A series of flight lines were flown over the Swan River on 18 February 1993. Weather conditions were acceptable, although the cloud that formed shortly afterwards limited some of the field spectral measurement program. Meteorological data and atmospheric profiles were obtained from the Perth Bureau of Meteorology. The flight lines were flown in both spectral and spatial modes. The "Scene Recovery Channel", which is included to view the area covered for the spectral-mode, was selected at band 210 (750 nm) to give good land/water comparisons. The spatial mode was selected to have 14 bands (listed in Table 1). On advice (*pers. comm.* D.L.B. Jupp CSIRO Div Water Res. Canberra) the analysis is only reported on bands beyond 500 nm because of low signal to noise ratio below that wavelength. This appeared to be sound advice, as high variability was shown in the early analyses; the authors believe that this problem has been solved in current configurations of CASI.

The CASI data were calibrated with a "flat-field" correction interpolating a reflectance line between a dark target (assumed zero) and a measured invariant target that was included in each flightline. We used a large area of a clear bitumen car park and compared it with a $BaSO_4$ standard plate.

## Field Measurements

The water column was sampled at the surface, 50 cm and 1 metre and then at 1 metre intervals to the bottom with a submersible pump. Phytoplankton were identified on the same day. Their cell densities were determined from samples preserved in lugol iodine with the aid of a 1 mL Sedgewick-Rafter counting chamber and an Olympus B-H-2 microscope at x 125 magnification. Salinity and temperature were measured with a Yeokal 602 meter (Hanon, Autolab, Sydney). Dissolved oxygen was measured *in situ* on a Yeokal 603 with salinity compensation. Secchi disc depths were estimated on the sunlit side of the boat, using a 200 mm diameter Secchi disc.

Chlorophyll was determined from phytoplankton cells filtered onto Whatman GF/C filter paper, stored frozen, and extracted by acetone after crushing. Spectrophotometry was done by standard methods of the Chemistry Centre of Western Australia (APHA - 18th ed.)

For the in-water spectral measurements, a water-tight radiometer housing with a clear perspex viewing window was mounted astern of the boat in a suspension frame. This enabled the DSIR radiometer within the housing to be pointed upward, with a diffuse filter, or downward for calculation of radiance or irradiance. The radiometer was lowered from a boom, clear of the stationary boat, to reduce the effect of shadowing or reflectance from the boat hull.

Spectral measurements were made just above the surface, and with the radiometer housing centred at 1 and 2 meters below the surface. The measurements were taken with the Mk2, DSIR Eight Channel Radiometer as close as possible to the flight times. The DSIR meter (Table 1) has narrow bands centred at 440(12.5), 480(9.5), 520(10.5), 560(9.5), 620(10.8), 670(11.5), 780(11.7) and 860(10.7) nm and a field of view of 20°. From these eight channels, an interpolation of a reflectance curve was possible.

## Analysis

A canonical variate analysis (CVA) was performed on all the data extracted from the CASI spatial image files for polygons (consisting of between 50 and 200 pixels). These were selected as close as could be identified to the monitoring sites, although Site Six was missed from one flight line through a navigation error, and Site Three was repeated with a second overlapping image. The aims of these statistical analyses were:

*(i)* to establish the relationship of the CASI data to the monitoring sites for which data on cell concentrations and water quality were available;
*(ii)* to determine whether the CASI spatial data could discriminate between bloom types that might bloom in the Swan/Canning system;
*(iii)* to determine which wavelengths, and how many, are required to describe water-column constituents; in particular, how well the existing bands in the DMSV perform compared with the full CASI data; and
*(iv)* to classify the river and nearby wetlands on the basis of the above analyses.

Briefly, a canonical variate analysis finds the linear combinations of the original variables (spectral bands) that maximise the differences between reference classes relative to the variation within the classes. Mathematically, this corresponds to finding linear combinations (canonical vectors) that maximise the ratio of the resulting between-groups to within-groups sum of squares for the resulting linear combinations. The canonical vectors give the directions of maximum class separability and the canonical roots give a measure of class separation in these directions. For a detailed description see, for example, Campbell and Atchely (1981) and Campbell (1984).

The river and wetland types were classified with a "maximum-likelihood" technique. This uses the combination of a predetermined number of bands that the CVA showed to provide maximum separation between all of the training sets (in this case all of the sampling sites), and allocates pixels to classes that are most like those known sites. Pixels in the image that fell outside class groups were not allocated.

# Results

## DSIR Data

The first objective was to compare the relationship of the in-water spectral measurements to the CASI high-resolution (288-band) data. Unfortunately, because the time taken for field measurements was significantly longer than the flights, simultaneous spectral measurements were possible for only two of the monitoring sites. During the morning of the overflight of CASI, cloud formed over the area and curtailed further measurement.

Figures 4 and 5 are DSIR meter spectra for Sites 1 and 2 respectively. The relative reflectance was calculated from the ratio of the upward to the downward position for each depth. The surface spectra (the unbroken line with Standard Error bars) show low relative reflectance (< 2%) below 500 nm and probably include a proportion of surface-skin scattering of sky radiance. At depth, the first two channels fall to zero, possibly because of absorption by the humic-rich (coffee-coloured) water of the Swan River. A maximum peak occurs at 550 nm (> 3%) and the reflectance declines to near zero by 780 nm. Site 1 (Figure 4) had significantly lower cell counts of both dinophytes and cryptophytes (Table 2) than Site 2 (Figure 5), which responded with a relative increase at 550 nm and a decrease at 670 nm. The relevance of the low reflectance below 500nm, and the maximum slope change beyond the red (650-750 nm) are discussed later in the analysis of the CASI data.

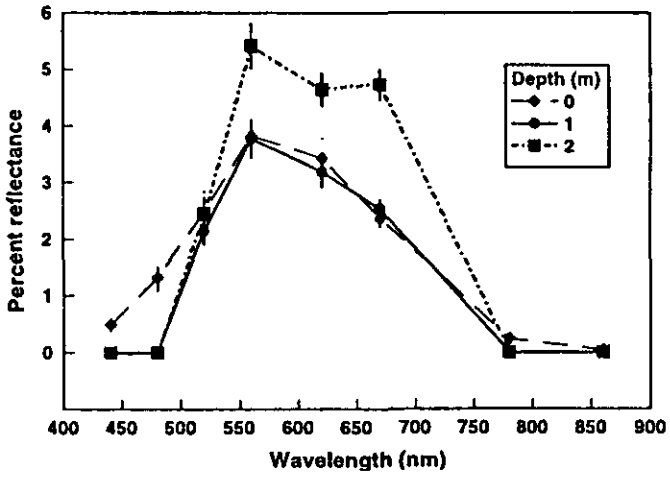


**Figure 4: DSIR meter spectra for Site 1**

*DSIR meter spectra for Site 1 (the Causeway) with the relative reflectance calculated from the ratio of the upward to the downward position for each depth.The surface spectra (the unbroken line) show very low relative reflectance below 500 nm, with a maximum at 550 nm and a decline to near zero by 780 nm.*

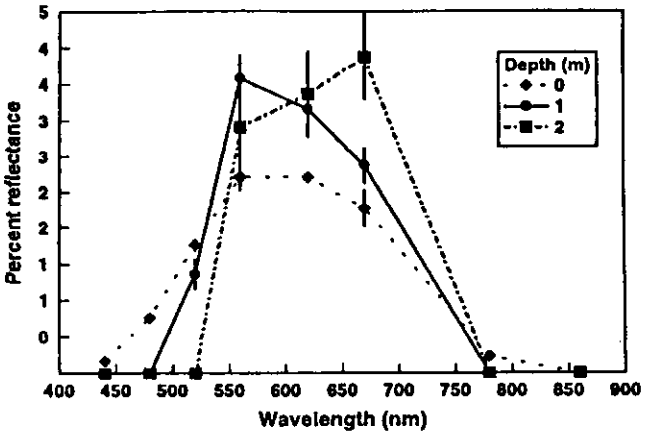


**Figure 5: DSIR meter spectra for Site 2**

*DSIR meter spectra for Site 2 (St Johns), which had significantly higher cell counts of both dinophytes and cryptophytes than Site 1 (Figure 4).*

The apparent increase in relative reflectance with depth is a function of the subsurface upward-to-downward ratio. This occurs as the irradiance (forward-scatter) becomes less, relative to the subsurface upwelling radiance (back-scatter). Note that the spectral-shape components are preserved. Note also that the Secchi extinction occurs at about 1-1.5 metres (Table 2), which indicates that total upwelling radiance is coming from within that range.

## Comparison of the Biological Data with Spectral-Mode CASI Data

The second objective was to measure the correlation of the biological measurements with the high-resolution CASI spectral measurements. Table 2 shows that the in-water measurements appear ranked in a one-dimensional direction upstream and many of the properties are highly correlated. This feature is caused by the incursion of saline marine water during the low-flow summer period.

Figure 6 shows the mean CASI spectral curves, extracted from the spectral-mode data, for the six monitoring sites in the Swan River. Unlike the DSIR in-water data, the spectral response is dominated by the atmosphere at the shorter (blue 400-500nm) wavelengths. However, a gradual decrease from the green (500-600nm) region through the red (600-700 nm) and a strong overall absorption into the reflected infrared is comparable up to about 750 nm. Beyond that wavelength the DSIR instrument provided no appreciable signal, but the CASI data contained the maximum spectral information for the separation of the sites.

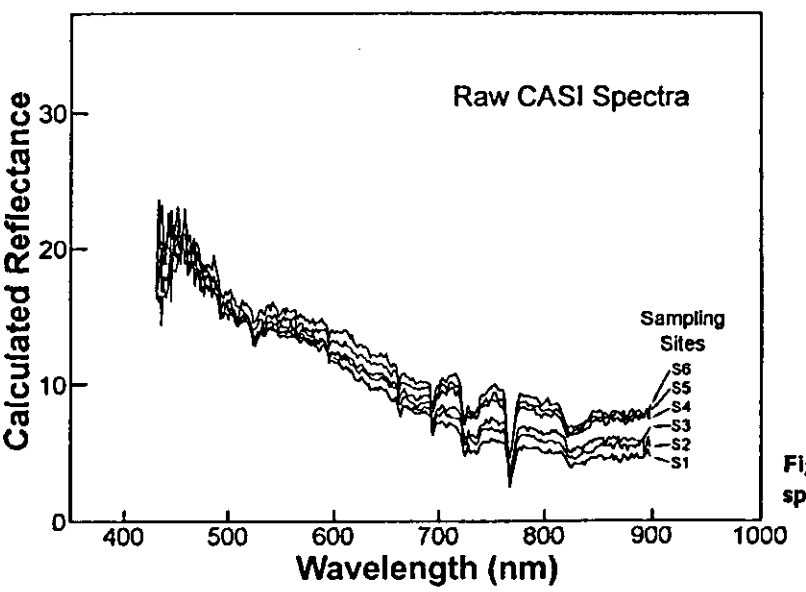


**Figure 6: CASI spectral curves**

*The mean CASI spectral curves, extracted from the spectral-mode data, for the six sites in the Swan River.*

The spectral feature of specific interest is the slight, but well-ordered, increase in red/infrared response corresponding with the increasing total cell counts and decrease in Secchi and salinity for the upstream sites. Table 2 summarises the surface to 0.5 m values for phytoplankton and pigments. This relationship of the CASI spectral data to the biological data was tested at 750nm.

Secchi disk readings and salinity were negatively related, but both showed a close relationship ($R^2$ of 0.87 and 0.95 respectively) to the spectral response and may reflect the saline incursion moving upstream. The relationship of total cells gave an $R^2$ of 0.94, and an even higher value was produced for the dominant cryptophyte *Cryptomonas* sp. The strong relationship was not supported by the dinoflagellates: the main species, *Gymnodinium* cf. *simplex* gave an $R^2$ value of only 0.44.

**Table 2 Chemical and biological measurements of the six monitoring sites on 18 February 1993**

| Site | Secchi (m) | Salt (Mg/L) | Chlor.a (Mg/L) | Chloro-phyta | Dyno-phyta | Crypto-phyta | Diatoms | Total Cells |
|---|---|---|---|---|---|---|---|---|
| 1. Causeway | 1.5 | 20.7 | 0.014 | 364 | 3569 | 72 | 34.3 | 5536 |
| 2. St Johns | 1.3 | 17.2 | 0.025 | 533 | 5370 | 1506 | 41.1 | 10880 |
| 3. Maylands | - | 16.7 | 0.006 | - | 1108 | 1918 | 73.0 | - |
| 4. White Rk | 0.9 | 13.4 | 0.049 | 728 | 15445 | 12239 | 13.3 | 30599 |
| 5. Kingsley | 1.0 | 11.5 | 0.046 | 582 | 11656 | 12676 | 5.2 | 26518 |
| 6. Success | 0.8 | 9.3 | 0.048 | 777 | 6977 | 20043 | 1.4 | 30421 |
| $R^2$ @ 750 nm | 0.87 | 0.95 | 0.77 | 0.70 | 0.44 | 0.95 | 0.59 | 0.94 |

The poor relationship of the dinophytes may be explained in part by the large variation in the biomass of the cryptophyte cells, which are 3-4 times larger than the dinoflagellate cells, thus producing biomass disparity of that order for the same cell count. Also, the density of these highly mobile organisms is hugely variable, especially early in the day. The relationship with chlorophyll-a, which is present in all phytoplankton, has an $R^2$ value of 0.77.

Figure 7 shows the plot of one of the monitoring sites (Site 2), and an adjacent wetland that at the time had a severe (probably *Anabaena* sp.) cyanobacterial bloom. The strong green peak (550-560nm) and a secondary chlorophyll peak closer to the infrared region are characteristic of pigments in cyanobacterial algae, which can grow at the low salinity extremes found in the upper Canning River and in the wetlands associated with the Swan River system.

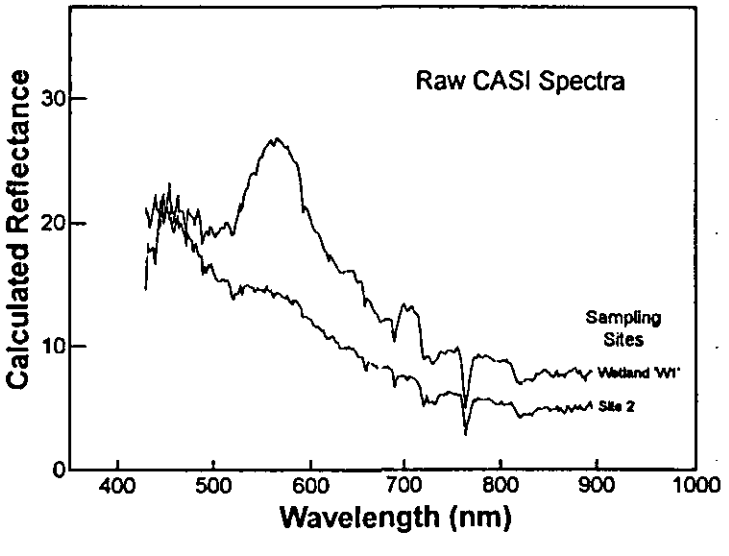


**Figure 7:CASI spectra for Site 2 and adjacent wetlands**

*The plots of one of the monitoring sites (Site 2) and one of the adjacent wetlands that was used in the classification; at the time, it had a severe cyanobacterial algae bloom. The strong green peak (550-560nm) and a secondary chlorophyll peak (700 nm) are characteristic of the extremes that occur in the Swan/Canning system.*

# Comparison of Biological Data with Spatial-Mode CASI Data

The third objective was to compare the Spatial-Mode (14-band) CASI data with the biological and physical measurements from the monitoring sites and from other areas with specific types of algal bloom using canonical variate analysis. The purpose was to determine which spectral regions, expressed as wavebands, can provide maximum separation between sites.

The first analysis was performed on training samples of polygons selected as close as could be identified in the image to the river monitoring sites. Site 6 was not included in the spatial-mode image because of a navigational error on the return flight line. Site 3 is represented by two training samples. Figure 8 is the canonical variate means plot and Table 3 summarises the analysis. The size of the canonical roots indicate that the training samples are very different spectrally. The first canonical vector explained 95% of the variability in the training data.

**Table 3 The canonical roots from the canonical variate analysis of the CASI spatial-mode data, with bands 3-14 for river sites.**

| *Canonical roots (1-5)* | | | | | *Sum of roots* |
|---|---|---|---|---|---|
| 127.6 | 4.601 | 1.812 | 0.621 | 0.091 | 134.763 |
| *Canonical Vectors for CVA 1 and 2 for the 12 bands* | | | | | |
| -0.5330E-02 | -0.688E-02 | -0.9677E-02 | -0.6007E-02 | 0.1843E-02 | 0.6533E-02 |
| 0.8545E-02 | 0.6894E-02 | 0.7496E-02 | 0.1079E0-01 | 0.7746E-02 | 0.2091E-02 |
| | | | | | |
| 0.1623E-01 | 0.3929E-02 | -0.6082E-03 | -0.1010E-01 | -0.4104E-02 | -0.9043E-02 |
| -0.5041E-02 | -0.1312E-02 | 0.3826E-02 | 0.3418E-02 | 0.2514E-02 | 0.3684E-04 |

The second analysis includes an additional three training sites (plotted as W1, W2, W3) selected from the wetlands to represent cyanobacterial and green algal blooms. Figure 9 and Table 4 summarise the analysis. They show that the algal sites are very different spectrally from the river sites. The first canonical vector discriminates between the algal and river sites; the second maintains the ordination of the river sites.

**Table 4 The canonical roots from the canonical variate analysis of the CASI spatial-mode data using bands 3-14 for river and wetland sites.**

| *Canonical roots (1-5)* | | | | | *Sum of roots* |
|---|---|---|---|---|---|
| 544.1 | 72.23 | 13.37 | 1.842 | 0.221 | 679.829 |
| *Canonical Vectors for CVA 1 and 2 for the 12 bands.* | | | | | |
| -0.2244E-02 | 0.1603E-02 | 0.1266E-01 | 0.1954E-01 | 0.2345E-02 | -0.3871E-02 |
| -0.7422E-03 | -0.1430E-01 | 0.2114E-02 | -0.2928E-02 | -0.1337E-02 | -0.1664E-02 |
| | | | | | |
| -0.2663E-02 | -0.3171E-02 | -0.5866E-02 | -0.4353E-02 | -0.2448E-02 | 0.4591E-02 |
| 0.5424E-02 | 0.6037E-02 | 0.2098E-02 | 0.1091E-01 | 0.8324E-02 | 0.2471E-02 |

Figure 7 is CASI spectra from Site 2 and an adjacent, highly eutrophic, wetland that drains into the river. The spectra show the characteristic green peak near 550 nm and a secondary peak near 700 nm, which is consistent with a green algal bloom. Comparison with Figure 6 shows that the difference between the spectrum from the wetland and the river site is much greater than the variation in the spectra for the six river sites. This difference is reflected in the large first canonical root in the analysis; the second canonical variate is maintaining the separation of the "river-only" sites.

**Figure 10: CASI image of the Swan River, using the best possible subset of spectral bands**

**Figure 11: CASI Image of the Swan River, using only the simulated DMSV spectral bands**

*Figure 11 is the same CASI image as in Figure 10, but this time with the classes overlaid that were obtained by processing only the three CASI bands that correspond with the DMSV (i.e. CASI bands 5, 9, and 12). The differences between the class-label images are summarised in Table 7, which compares the site-by-site totals of the allocated pixels.*

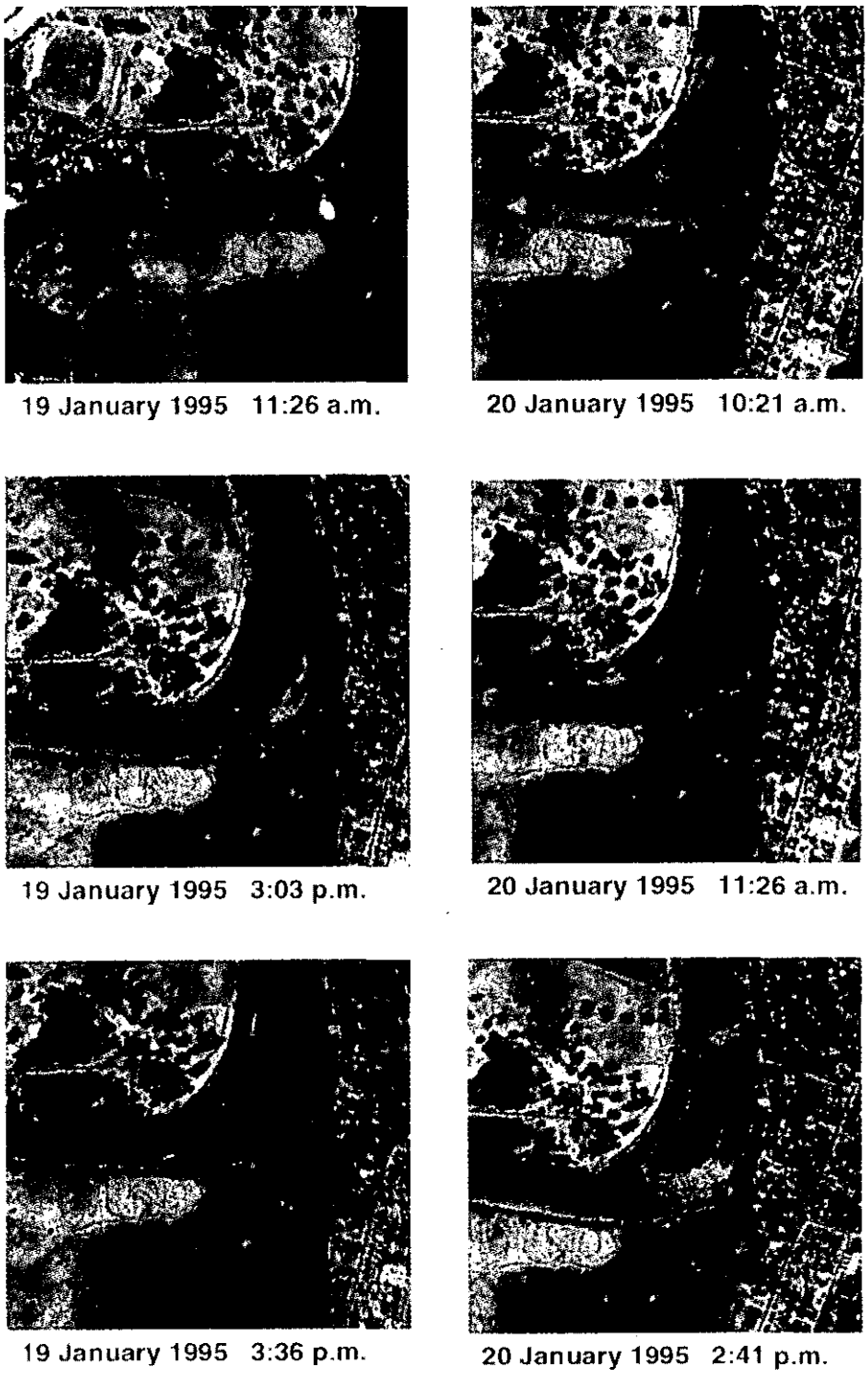


**Figure 15: Series of DMSV images**

*An example of the spatial and temporal variation in distribution of the algal bloom* Gymnodinium *(white-light purple shading) near Ron Courtney Island, Swan River, Western Australia.*


**Figure 18. A: DMSV image of Sandringham Jetty area showing the natural water colour of the Swan River. B: The same image enhanced to show hydrodynamic features and a *Eutreptiella* sp. algal bloom (in orange)**

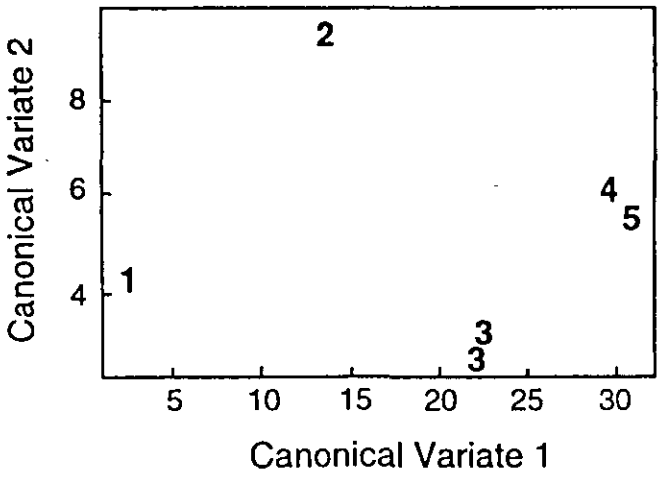


**Figure 8: Canonical Variate analysis for river sites**

*Plot of the first and second canonical vector of the group means of the CASI spatial-mode data, using bands 3-14 (Table 1) for five of the river-only sites.*

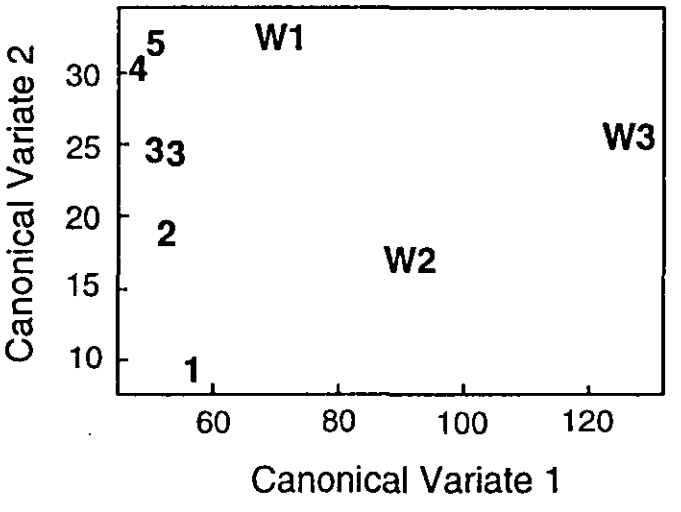


**Figure 9: Canonical Variate analysis for river and wetland Sites**

*Plot of the first and second canonical vector of the group means of the CASI spatial-mode data using bands 3-14 (Table 1) for the five river sites and the three adjacent wetland sites.*

To determine which spectral bands are important, and in what order of importance, a variable selection procedure was applied to the data. Table 5 is a summary of the results when applied to the river-only sites. It shows that as few as three bands can maintain 75% of the separation of the training samples. These bands are 3 (497-504 nm, a chlorophyll band), 6 (564-572 nm, the pigment phycoethrin) and 12 (746-755nm, the infrared); see Table 1.

Table 6 summarises the results of the variable selection procedure applied to the combination of the river and wetland sites with algal blooms. In this case a contrast vector was used to focus on the most important bands for separating the algal bloom sites from the river sites. The important band combinations are related to those for discriminating between the river sites. The most obvious changes are the increased importance of band 5 and the decreased importance of band 12. Three bands — 5, 6 and 10 — explain 95% of the separation between the algal and river sites, which is sufficient to map the variation.

**Table 5 River sites only: the discriminant indices for optimum separation uses a variable selection procedure for 1 to 12 bands. The cumulative percentage is based on the proportion of separation possible if all bands are used.**

| *Size of Band Subset* | *Best Band Combination* | *log (det (W)/ det W+B)* | *%* |
|---|---|---|---|
| 1 | 12 | 3.98 | 48.5 |
| 2 | 3,12 | 5.23 | 64.8 |
| 3 | 3,6,12 | 6.20 | 75.6 |
| 4 | 3,6,11,12 | 6.78 | 82.7 |
| 5 | 3,6,10-12 | 7.19 | 87.1 |
| 6 | 3,6,7,10-12 | 7.50 | 91.5 |
| 7 | 3,6,7,10-13 | 7.67 | 93.5 |
| 8 | 3,4,6,7,10-13 | 7.84 | 95.6 |
| 9 | 3-7,10-13 | 7.97 | 97.2 |
| 10 | 3-7,9-13 | 8.08 | 98.5 |
| 11 | 3-13 | 8.14 | 99.3 |
| 12 | 3-14 | 8.20 | 100 |

**Table 6 River and wetland sites: The discriminant indices for optimum separation uses a variable selection procedure for 1 to 12 bands. The cumulative percentage is based on the proportion of separation possible if all bands are used**

| *Size of Band Subset* | *Best Band Combination* | *log (det (W)/ det W+B)* | *%* |
|---|---|---|---|
| 1 | 6 | 2.37 | 66.0 |
| 2 | 6,10 | 2.83 | 78.8 |
| 3* | 5,6,10 | 3.40 | 94.7 |
| 4 | 5,6,8,10 | 3.45 | 96.1 |
| 5 | 5,6,8,10,14 | 3.51 | 97.8 |
| 6 | 3,5,6,8,10,14 | 3.53 | 98.3 |
| 7 | 3,5,6,8,10,11,14 | 3.56 | 99.2 |
| 8 | 3-6,8,10,11,14 | 3.57 | 99.4 |
| 9 | 3-6,8,10-12,14 | 3.59 | 100 |
| 10 | 3-6,8-13,14 | 3.59 | 100 |
| 11 | 3-12,14 | 3.59 | 100 |
| 12 | 3-14 | 3.59 | 100 |

## Image Classification

Maximum likelihood classification (Figure 9) was used to match the rest of the image pixels to the training samples that represented the river sites and the adjacent wetlands. A subset of the spectral bands was chosen for use in the calculations. These bands — 3, 5, 6, 7, 10, 11, and 12 — were selected in the previous analysis as the best bands to both discriminate between the river sites (six bands — 3, 6, 7, 10, 11 and 12) and to separate the wetland algal bloom sites (three bands — 5, 6 and 10) from the river sites.

Figure 10 (see page 19) is the CASI image with the classification overlaid. The image has been corrected for aircraft roll and calibrated to reflectances. The river pixels that have not been assigned to one of the classes are affected by sunglint. No attempt has been made to remove this effect, although the qualitatively effective technique of Ong et al. (1994) could have been applied; however, its effect on the classification could have been misleading.

## Simulation of Simple Multi-Band Video System

The simulation was done on the four-band SpecTerra DMSV system. The bands in this system were specifically chosen by the manufacturer for imaging terrestrial vegetation but significant information on the pigments in the Swan River has been clearly evident in recently flown images. To assess the usefulness of these four bands, canonical variate analyses have also been performed to determine the spectral separability of both the river monitoring sites and the wetland algal bloom sites using the CASI bands that most closely represent the DMSV bands (see Table 1).

The analysis was performed in the following ways. Firstly, bands 1, 5, 9 and 12 were compared with 1, 5, 9 and 13 because the DMSV band 4 lies between the CASI bands 12 and 13. The sum of roots varied only slightly and the band combination accounted for 57% and 52% respectively of the total separation provided when all bands were used. Therefore band 12 was chosen, as it is spectrally closer to band 4 and also gave the higher value. Secondly, to be consistent with the analysis of the CASI data (omission of data below 500 nm), the CVA was re-run omitting band one (leaving bands 5, 9 and 12), which then accounted for 55% of the maximum possible separation achieved with all 12 CASI bands.

**Table 7: Comparison of the concurrence of classes allocated by the best subset of seven CASI bands against those allocated by the three CASI bands that most closely correspond with those of the DMSV system.**

| | CASI Classification | | | | | | | | |
|---|---|---|---|---|---|---|---|---|---|
| | *site 1* | *site 2* | *site 3* | *site 4* | *site 5* | *W1* | *W2* | *W3* | *Uncl* |
| *site 1* | 11215 | 969 | 439 | 0 | 0 | 0 | 0 | 0 | 251 |
| *site 2* | 811 | 10820 | 3276 | 4 | 0 | 3 | 0 | 0 | 71 |
| *site 3* | 18 | 1877 | 15924 | 153 | 787 | 12 | 0 | 0 | 7460 |
| *site 4* | 0 | 0 | 76 | 2160 | 282 | 0 | 0 | 0 | 1 |
| *site 5* | 0 | 9 | 37 | 750 | 19404 | 2 | 0 | 0 | 7811 |
| *W1* | 0 | 0 | 4 | 0 | 33 | 1642 | 0 | 8 | 2531 |
| *W2* | 0 | 0 | 0 | 0 | 0 | 0 | 666 | 0 | 1082 |
| *W3* | 0 | 0 | 0 | 0 | 0 | 0 | 0 | 3797 | 2971 |
| *Uncl* | 0 | 0 | 0 | 0 | 0 | 0 | 0 | 0 | 1903656 |

In effect, if a pixel that was allocated to site *n* by using the best subset of CASI bands also was allocated to site *n* by using the best subset of DMSV-equivalent bands it, is said to concur. If the allocation moved to the adjacent site or sites, it is considered as drift. For example, 666 pixels were allocated to site W2 by the CASI subset, and all those pixels were correctly allocated by the best subset of DMSV-equivalent bands; in contrast, 19404 pixels were correctly allocated to site 5, but about 1000 drifted to the adjacent sites 3, 4 and W1.

The separation of the six sample sites by the best subset of all CASI bands is good (bands 3, 6, 7, 10, 11 and 12 giving 91.5% of separation). The three-band combination of DMSV-equivalent bands (bands 5, 9 and 12, which accounted for only 55% of that separation), is giving a highly comparable result. The cross-aggregation shows that the three DMSV equivalent bands are also able to separate the algal blooms in the wetlands. Drift to other adjacent river classes is less than an average of 15%. When the comparison of the likely separation of the best-subset and the DMSV-equivalent bands is made with the cyanobacterial algal blooms (W1, W2 and W3), there is concurrence in more than 99% of pixels.

From this analysis it is reasonable to assume that the next stage is to test the best-bands selection from the CASI analysis in the DMSV. The choice of the four best bands would be to use the combination of CASI bands 5, 6, 8 and 10. This relates to using narrow wavebands centred on about 550, 570, 625 and 670 nm.

# Discussion and Conclusions

The examples in this study clearly show what the CASI instrument does well. It is sensitive to spectral features of low to moderate concentrations of algal bloom types and other co-varying parameters. The very high spectral resolution will undoubtedly give great confidence to the selection of diagnostic wavelengths for the remote sensing of water-quality parameters.

This study also emphasises the difficulty of obtaining spectral measurements of the water column by conventional field methods. This very important aspect requires further research and instrument development.

However, the real issue is: how few bands, and how broad can those band can be, to still retain reliable diagnostic information. Recent laboratory studies by Johnsen et al. (1994) concluded that, for the 10 main classes of phytoplankton covering 31 algal bloom species that they studied (most of which are in the Swan system), a set of only 3-5 wavelengths yielded near-optimum classification success. The challenge is to transfer that success to remote sensing systems in the field.

This study shows that the classification of water bodies with low to moderate concentrations of phytoplankton within the range covered by the six river monitoring sites is possible, but is probably influenced by co-varying parameters such as salinity and turbidity. Correlations to cell counts of better than $R^2 = 0.9$ are presented for the limited extent of this study. The domination of the spectral response by the humic component needs to be considered if low concentrations of bloom types are to be sensed, but where major blooms are likely, this analysis demonstrates that spectral separation is possible. To discriminate between bloom types in the main groups of chlorophytes, cryptophytes and diatoms may also be possible with a limited number of bands.

When the comparison of the separation of the best-subset of all CASI bands and the DMSV-like bands is made only with cyanobacteria in the wetland sites there is concurrence in better than 99% of cases. The cross-aggregation shows that the three DMSV-like bands are able to separate the algae in the wetlands from the river sites with very high reliability; drifts to adjacent river-only classes are fewer than an average of 15%.

Delays in the arrival of the CASI instrument unfortunately meant that by February the most severe algal blooms in the Swan River which occur in spring and early summer, were finished, as the river had become more saline from marine incursions. For monitoring the widely scattered water bodies in Western Australia it is likely that a simple low-cost airborne system with as few as 3-4 well-chosen bands could provide the spectral requirements for detection of blooms if supported with some in-water calibration. It then becomes an economic question as to how often the bloom is monitored.

# DMSV Related Studies

The work with CASI and other baseline spectral sampling highlighted the logistical difficulties of gathering information in the field to cover a sufficiently large area within the flight times.

The number of potentially confounding factors makes collection of ground-truth data essential to calibrate remotely sensed images and their algorithms (Jupp et al., 1994). While these data can be used to calibrate models, the highly dynamic nature of algal blooms, and their variability in space and time, requires ground-truthing collection times to be as close as possible to the remote sensing flight. This may not always be practicable, so it may be necessary to sample to confirm the reliability of algorithms developed for other locations or times.

The aim of this work was to assess the short-term spatial and temporal variation in bloom dynamics and its implication for the timing of ground-truthing of data acquired by digital multispectral video.

## Methods

During 1994-95, Perth experienced its driest spring, summer and autumn for over 100 years. Thus, far fewer nutrients were washed into the river and blooms were much smaller than in other years.

Despite the lack of rain and catchment-related nutrient input in the Swan River during the summer of 1995, a small bloom of the dinoflagellate *Gymnodinium* cf. *simplex*

occurred in mid-January. *Gymnodinium* usually forms large monospecific blooms every year , generally between January and April. It is a mobile alga, with flagella that enable it to change its vertical distribution in the water column, presumably in response to changes in environmental parameters, such as nutrients and light.

## Ground-Truthing

Sampling sites were recorded automatically by a GPS logged to a laptop computer. They were further fixed by the siting of at least three landward bearings from the boat and the location of the boat, with respect to land features was drawn on an aerial photograph of the section of river to ensure each sampling site was accurately located. Data collected are shown in Table 8.

**Table 8: Ground-truthing Data Collected during the Study; n = number of replicates**

| *Data collected during ground-truthing (Parameter)* | *Depth (m)* | *n* | *Times per day* |
|---|---|---|---|
| In vivo fluorescence calibrated to yield chlorophyll *a* in µg $L^{-1}$ | < 0.25 | 5 | 3-4 |
| In vivo fluorescence calibrated to yield chlorophyll *a* in µg $L^{-1}$ | 0.5 | 5 | 3-4 |
| In vivo fluorescence calibrated to yield chlorophyll *a* in µg $L^{-1}$ | 1.0 | 5 | 3-4 |
| Total suspended solids (mg $L^{-1}$) | < 0.25 | 5 | 3-4 |
| Secchi depth (m) | variable | 1 | 3-4 |
| Current speed & direction (m $s^{-1}$) | 1.0 | 1 | 3-4 |
| Wind speed & direction (knots) | – | 1 | 3-4 |
| Chlorophyll *a*, *b*, *c* & phaeophytin (µg $L^{-1}$) | < 0.25 | 5 | 1-1 |
| Spectral transmission of unfiltered water | < 0.25 | 5 | 1-1 |
| Spectral transmission of GFC-filtered water (=1µm) | < 0.25 | 5 | 1-1 |
| Spectral transmission of 0.2 µm membrane-filtered water | < 0.25 | 5 | 1-1 |
| Phytoplankton identification | < 0.25 | 5 | 1-1 |
| Cell count (cells $mL^{-1}$) | < 0.25 | 5 | 1-1 |

### Chlorophyll Fluorescence

A Turner fluorometer, logged by a laptop computer, recorded *in vivo* fluorescence which was converted to a reading of chlorophyll (Figure 12). Samples were pumped on board the boat and through the fluorometer from a darkened intake tube that could be moved vertically in the water column to sample at different depths. The default sampling depth was 0.25 m while the boat was moving between ground-truthing sites, and samples were taken at < 0.25 m, 0.5 m, and 1 m depths at each ground-truthing site. Sampling sites that had approximately 20%, 40%, 60%, 80% and 100% (log scale) of the maximum chlorophyll concentration for each day were selected to provide a range of chlorophyll values on which to calibrate airborne data. A minimum of 5 replicates of each sample was taken for each bloom concentration at 3 depths within the water column: surface (< 0.25 m) 0.5 m and 1.0 m.

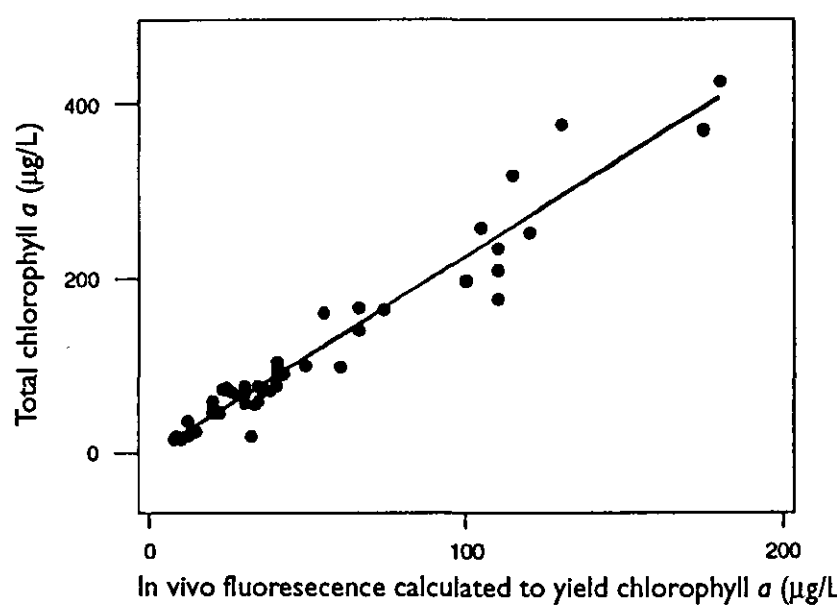


**Figure 12 Relationship between total chlorophyll and *in vivo* fluorescence**

### Chlorophyll Determinations From Filtered Samples

Samples for analysing chlorophyll *a*, *b* and *c*, and phaeophytin taken from <0.25 m depth were filtered through a 0.8-1.2 mm GFC filter. The filter paper, with filtered material, was stored on ice in a completely darkened, insulated container until the samples were taken to the laboratory (within one hour of collection of the last sample for that overflight). Data from the first and last day of the study (i.e. 18 and 20 January 1995) were used to calibrate the fluorescence samples from the Turner fluorometer. There was a very good linear relationship between total chlorophyll and fluorescence (Figure 11 (see page 20): $R^2 = 0.94$, $n = 50$; $P < 0.001$) indicating that more rapid measurement of fluorometry could reliably be used to estimate chlorophyll of the algal bloom.

### Spectral Measurements

Reflectance spectra of *Gymnodinium* at cell concentrations of 7,300, 28,000 and 47,700 cells $mL^{-1}$ were measured on filter papers, using an Ocean Optics miniature field spectrometer covering 360-860 nm. Water samples, also collected for spectral scans, were stored in an iced-chilled container for transportation to the laboratory. Samples of unfiltered, filtered through a 0.0.8-1.2µm GFC filter or a 0.2 µm membrane filter were scanned between 300 and 900 nm for transmission spectra using a VARIAN spectrophotometer.

### Water Clarity

An index of water clarity was made by using a Secchi disk at each ground-truthing station and determining the total suspended solids (>0.45 mm) from 1 litre samples taken at the same time.

### Water movement

The speed and direction of the river current were estimated by measuring the distance that a subsurface drogue set at 1 m depth (with a small surface float) travelled over a set interval of time.

### Biological Samples

The species and density of cells were measured in the laboratory from field samples to which a Lugol preservative had been added.

## Airborne Data Collection

The DMSV was installed in a light aircraft and flight plans were lodged for three days of missions over the Swan River in the metropolitan area of Perth. The part of the river that was reported to have shown evidence of the bloom was divided into eight flightlines of about 50 DMSV frames each covering about 1 $km^2$. Spatial resolution was set at a nominal pixel size of 1.5 m x 1.5m (flying height 2200 m above ground) and frames were taken with a 50% overlap; only the portions of the image unaffected by sunglint were used.

Waypoints for navigation were recorded into a GPS before the flights. Flight times were scheduled for 10.00, 12.00, 14.00 and 16.00 h,. with in-water sampling planned to coincide with each flight (= 45 minute duration). The flight lines were adjusted to give optimum coverage of the bloom range in the river by communications between the aircrew and the boat crew.

### Digital Multi-Spectral Video

The Digital Multi-Spectral Video (DMSV) is a four-camera (CCD-array) which frame-grabs and digitises images for instant display or storage for further processing (Lyon et al. 1994). Filters for narrow-band interference filters at the wave-centres of 450 nm, 550 nm, 650 nm and 770 nm are attached to each camera. The spatial resolution, as a function of flying height, can vary from 30 cm to 3 m. Filters can be changed, to provide a choice of optimum wavelengths for different bloom types, is an attractive feature when detecting algal blooms containing different pigments. Unfortunately, it was not possible to test an alternate selection of filters during this study.

### Calibration of DMSV Data to Reflectance

To compare data from each flight time, and to compare imagery from previous missions, it is essential to calibrate DMSV data. Illumination conditions may vary, and gains and offsets are normally set at the beginning of each flight to optimise the dynamic range of the 8-bit data, but are not changed during the flight.

The method of calibration used to transform raw data to reflectance was a modified "flat-field" correction (Hick et al., 1994). The range of reflectances that are of interest in algal bloom studies in the river are between 1 and 8% (Hick and Jernakoff, 1994), and fringing vegetation are of the order of 30%. A target at each end of this range was used to estimate the calibration line. The invariant standard target on the apron and runway of Perth International Airport was approximately 20% reflectance. The shadow of bridges and other fixed structures were assumed to have the lowest reflectance value in the range of interest. The zero value was estimated at 90% of these values.

## Image Rectification

DMSV images were georeferenced to a SPOT panchromatic satellite image. The usual spatial resolution, or pixel size, chosen for DMSV data is around one to about two metres, while SPOT panchromatic data have a nominal ground resolution of ten metres. The linear fit of the DMSV data to the SPOT image is based on the minimum number of ground control points that will give subpixel precision of panchromatic data, selected where possible in each corner of each frame. Each DMSV image is then "stitched" into the image framework.

## Image Analysis

The position of each in-water sampling site was located on the image and the calibrated four-band digital data for that site were extracted for analysis. Sites that were sampled more than 20-25 minutes before or after the flight times were omitted from the analysis. River current and wind conditions were accounted for during the selection of data polygons and, where possible, the selected areas were in close concurrence to the sampled position.

The analysis included linear regressions of the fluorometer data with individual bands and various combinations of band ratios. This was done for all sites grouped as a whole, for all sites on each day, and for the combined sites flown in the mornings and afternoons. "Out of range" data from sites with high solar angles were omitted.

# Results

## Ground-truthing

### Composition of the Algal Bloom Types

The algal bloom mainly consisted of the dinoflagellate, *Gymnodinium* cf. *simplex*. Cryptophytes and chlorophytes contributed less than 15% of the total number of cells in the bloom (Figure 13).

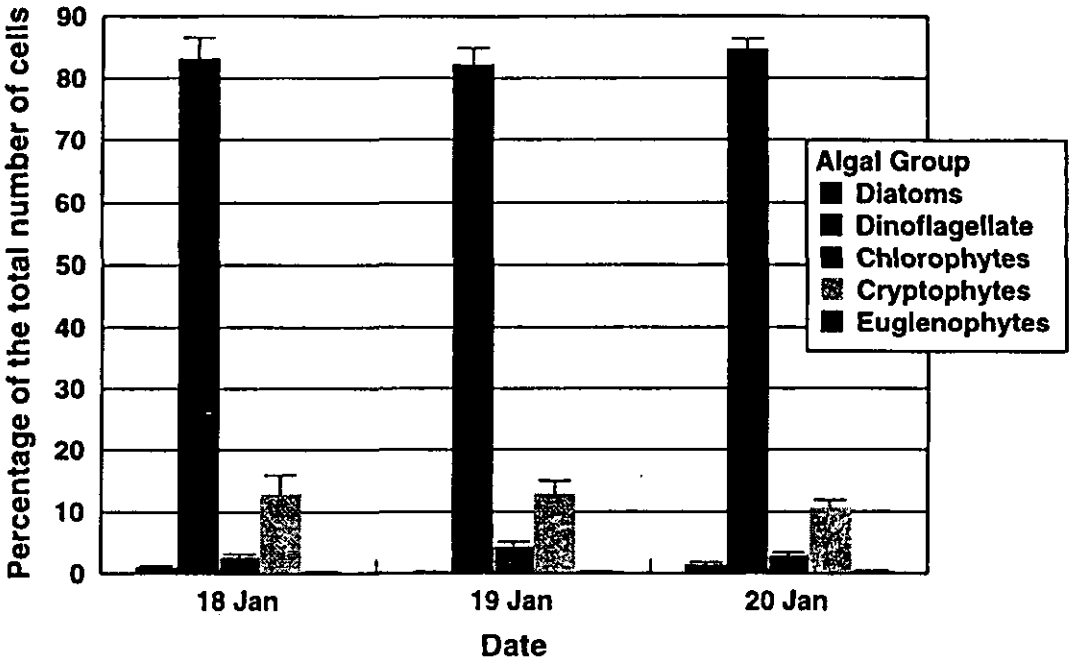


**Figure 13: Percent composition of algal cells**
*Mean percent composition (± SE) of algal groups within the bloom (Data Pooled over Sites).*

### Composition Of Bloom Pigments

The proportion of bloom pigments was relatively constant throughout the study indicating that no major life-cycle changes happened during the study e.g. bloom death, which would be indicated by an increase in phaeophytin. Over the three days, the percent of the total pigment concentration was 77.3 % (+ 0.9%) for chlorophyll *a*, 1.9% (± 0.2%) for chlorophyll *b*, 18.2% (± 0.7%) for chlorophyll *c*, and 2.6% (± 0.4%) for phaeophytin levels.

### Spatial, Temporal and Depth Variability in Algal Bloom Chlorophyll

The distribution of the bloom at the study site, as measured by fluorescence, varied within and between days and depths within the water column (Figure 14). In general, there were more phytoplankton in surface waters in the mid- to late afternoon than at other times. Data (pooled within and between days) indicated that values at the water surface values ranged from 7.5 $\mu g\ L^{-1}$ to 340.0 $\mu g\ L^{-1}$ while at 0.5 m they ranged from 8.5 $\mu g\ L^{-1}$ to 270.0 $\mu g\ L^{-1}$ and at 1 m depth they ranged from 12.0 $\mu g\ L^{-1}$ to 125.0 $\mu g\ L^{-1}$ .

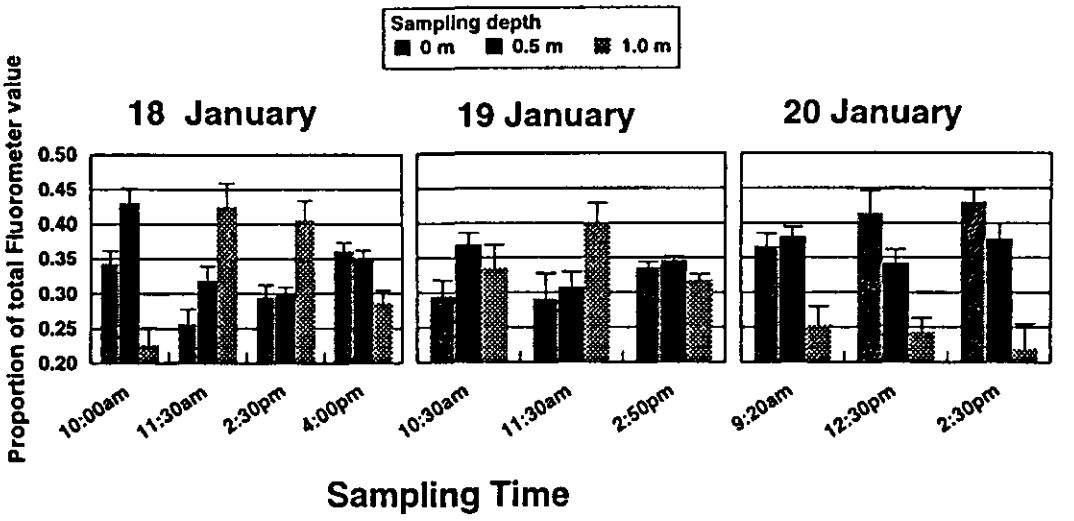


**Figure 14: Proportion of total bloom concentrations**
*Mean (± SE) Proportion of the Total Bloom Concentration (Data Pooled over Sites).*

The series of DMSV images provide qualitative information on the dynamics of water column constituents. Figure 15 (see page 21) is an example of six, single, calibrated DMSV frames that show the spatial and temporal variation in bloom dynamics taken of an area near Ron Courtney Island at 11.26 a.m., 3.03 p.m. and 3.36 p.m. on Thursday 19 January; and at 10.21 a.m., 11.26 a.m., and 2.20 p.m. on Friday 20 January, 1995. Spatial and temporal variation in bloom distribution is evident. Some of the effects of sunglint (caused by winds gusting to greater than 20 km h-1 causing wave-facets) have been removed from the images before mosaicing the flight lines.

The areas for which in-water data are available lie within these images. The areas where visible and fluorometrically measurable blooms occurred appear as lighter areas in these enhancements (11.26 a.m., 19 February). These images show that the distribution of algal blooms within the same area of the river varies substantially within a day and between days. These images also show that the areas suspected of having the highest concentrations do not persist for long periods (11.26 a.m., 19 February). Overturn of water caused by the passage of a boat can be seen in some images, and this feature was readily observed by the boat crew (e.g. 11.26 a.m., 19 February).

## Secchi Disk Index of Light Penetration

While Secchi depth limits were from a minimum of 0.2 m to a maximum of 1.0 m, the overall average Secchi depth was 0.48 m (± 0.02 m) during the study. It was unlikely, therefore, that the DMSV could detect phytoplankton below 0.5 m depth. More specifically, Secchi readings were relatively consistent between sampling times on 18 January, but on 19 and 20 January there was a marked decrease in light penetration in the afternoon sampling period (Figure 16) which corresponded with the increased levels of chlorophyll in the upper water column (Figure 14).

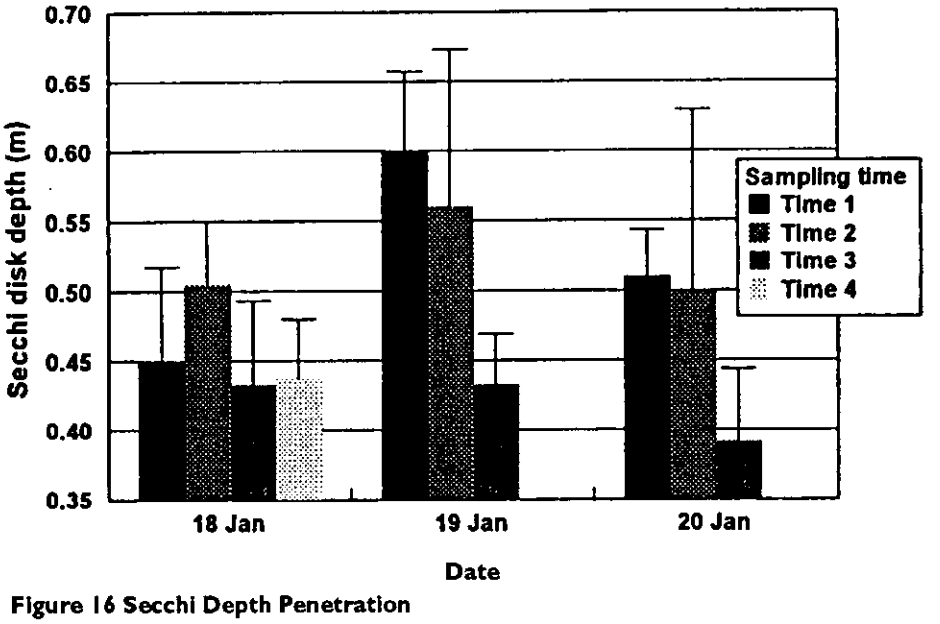


**Figure 16 Secchi Depth Penetration**

### Total Suspended Solids

The level of total suspended solids was significantly higher on 20 January (33.28 mg $L^{-1}$ ± 0.60 mg $L^{-1}$) than on either 18 (27.24 mg $L^{-1}$ ± 0.92 mg $L^{-1}$) or 19 January (26.83 mg $L^{-1}$ ± 0.91 mg $L^{-1}$); analysis of variance, df = 2,70, P < 0.001) 18 and 19 respectively). This difference was believed to be caused by wind disturbing the water column and stirring up sediments (average wind over the study sites was estimated to be 4 knots on 18 and 19 January and 10 knots with strong gusts on 20 January).

### Relationship between Chlorophyll, Secchi Depth and Total Suspended Solids

The influence of chlorophyll content and total suspended solids within the top 0.5 m on light levels (as measured by Secchi depth penetration), was variable between days.

On 18 January, chlorophyll alone showed a significant negative relationship with Secchi depth ($R^2$= 0.81, n = 25; P < 0.001). This relationship was improved by including the total suspended solids in a multiple regression (R2= 0.89, n = 25, P<0.001): Secchi = 0.657 - 1.03 x Log (Chlorophyll) + 0.00001 x Total Suspended Solids. The contribution of chlorophyll explained 91% (of the total sum of squares) of the significant regression, whereas by the level of total suspended solids explained only 9%. This suggested that, for this particular day, bloom cells were the main water-column constituent influencing light levels in the river.

On 19 January some Secchi data were identified as being incorrectly recorded and were removed from the subsequent analyses. Chlorophyll alone showed a significant negative relationship with Secchi depth (R2 = 0.41, n = 18; P < 0.001). Once again, this relationship was improved by the addition of the total suspended solids in a multiple regression (R2= 0.75, n = 18, P < 0.001); Secchi = 0.632 - 0.141 Log (Chlorophyll) + 0.000017 x Total Suspended Solids. The contribution of chlorophyll explained 55% of the significant regression, while the total suspended solids explained 45%.

On the 20 January chlorophyll alone showed a significant positive relationship with Secchi (R2=0.71, n = 25, P < 0.001), which was only slightly improved by adding the total suspended solids ($R^2$= 0.79, n = 25, P<0.001); Secchi = 0.351 + 0.0967 x Log (Chlorophyll) - 0.000006 x Total Suspended Solids. The contribution of chlorophyll explained 90% (of the total sum of squares) of the significant regression, whereas the total suspended solids explained only 10%. It is of interest to note that, while there was a negative relationship between Secchi and chlorophyll on 18 and 19 January, the relationship on 20 January was positive. Furthermore, the only occasion where the amount of chlorophyll correlated with the level of total suspended solids was on 20 January (correlation coefficient = -0.676; n = 25, P<0.01).

These relationships highlight the highly dynamic and complex nature of the water column constituents of the Swan River.

## Spectral Characteristics Of Gymnodinium

The spectra in Figure 17 are dominated (98% of cells) by the dinoflagellate *Gymnodinium* cf. *simplex*, which has a mixture of pigments, resulting in its brown-orange colour. It also has characteristic spectral features of chlorophyll a (generally below 500 nm, with B-carotene above 500 nm and other chlorophyll pigments contributing to the shape of the reflectance curve between 660 and 700nm.

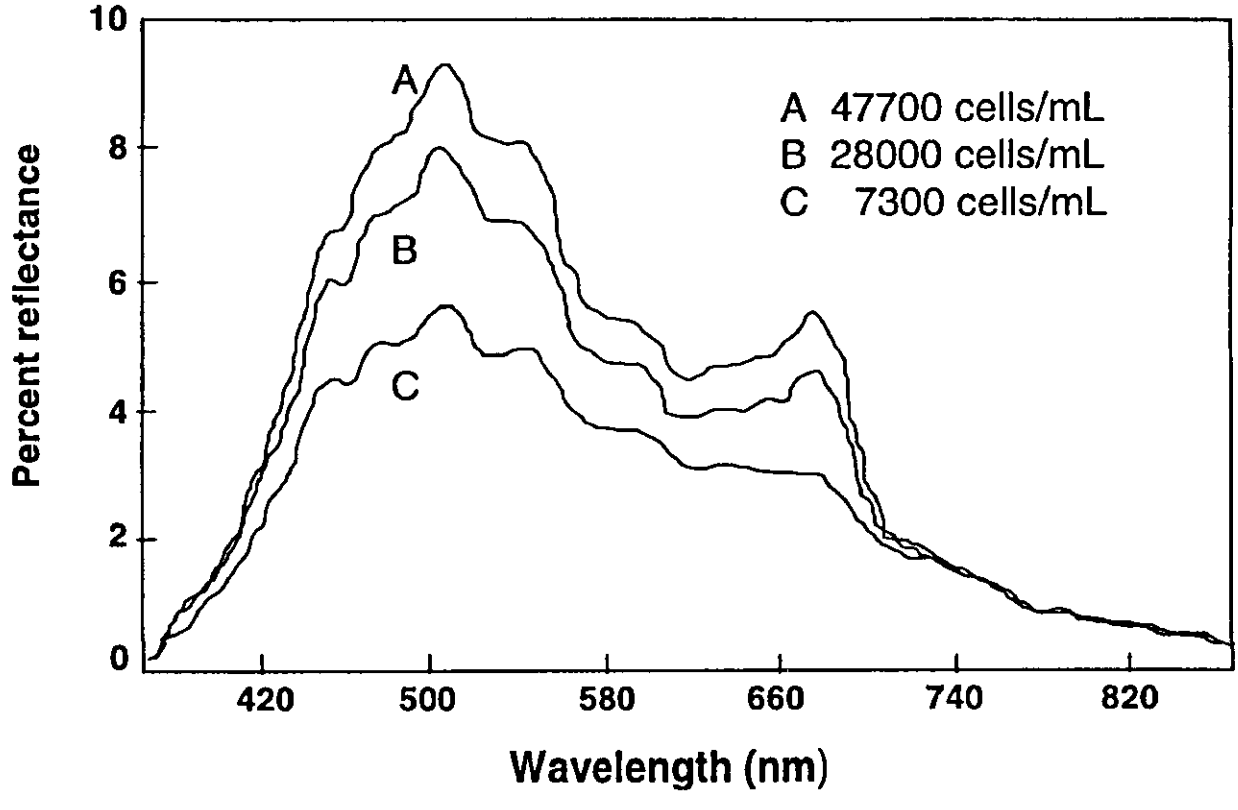


**Figure 17: Reflectance spectra of *Gymnodinium* at three concentrations**
*DMSV Data Compared with Algal Bloom Concentration*

A hardware malfunction in the DMSV on 18 January lost most of the video data for that day. However, on that and the other two days, a total of 27 sites had been field-sampled within 45 minutes of the overpasses of the DMSV.

There was no combination of bands, or a single band, that gave a consistently good relationship to fluorometer measurements across all times and days. The best regression was against band ratios of b1/b2 ($R^2$ = 0.58, n = 13, P = 0.002) on 19 January, but this good relationship of b1/b2 was not consistent on the other two days ($R^2$ = 0.36, n = 6, P = 0.211) and ($R^2$ = 0.11, n = 5, P = 0.594). The best band combination on 18 January was b2/b3 ($R^2$ = 0.47, n = 6, P = 0.135) and b2/b4 ($R^2$ =

0.37, n = 5, P = 0.274) on 20 January. There was a poorer relationship when all the days were combined and when the mornings and afternoons were compared. The best relationship for fluorescence for morning data was for the ratio of bands b2/b3 ($R^2$ = 0.004, n = 17, P = 0.801). With the afternoon data, the best relationship was obtained from the ratio of bands 1/3 ($R^2$ = 0.54, n = 10, P= 0.015). Thus, a significant regression was only apparent with the afternoon data (which was also when more phytoplankton tended to be in surface waters; Figure 14).

# Discussion and Conclusions

Algal blooms such as *Gymnodinium* are dynamic in both space and time. Although this study was unable to determine whether the bloom's temporal and spatial patchiness was caused by horizontal advection or vertical migration of the phytoplankton cells (or a combination), it has highlighted the need to take account of this variability when using water samples for calibrate and validate of remotely sensed data.

Regardless of the reason for the bloom patchiness, the study indicates the need to ensure the water is sampled within a short time of the overflight. It also highlighted the problems of collecting enough water samples within the restricted time. The small number of samples taken at some sites and times during the overflight period may be the reason several expected trends in the data (see Results) were not clear. A better approach to obtain more samples within a short time would be to use several fluorometers simultaneously.

In the present study, the 1.5 m x 1.5 m pixel size provided good discrimination of bloom distribution within the Swan River. It also allowed several replicate pixels within the images to be measured for analyses and interpretation, and it was possible to sample in the field at a similar spatial scale.

The use of remote sensing to detect and quantify algal blooms requires that a relationship exists between in-water data and the remotely sensed image. Although the detection of, for example, cyanobacteria blooms in our and in other studies has been highly successful because of the algae's distinctive spectral pigments (Jupp et al., 1994), detection of the brown-pigmented dinoflagellates is more difficult, especially in the humic waters of the Swan River. Earlier in this study, we found a variable relationship between spectral bands on CASI and the type of phytoplankton blooming. It was strong between spectral bands and cell count for the dominant cryptophyte, *Cryptomonas* sp., which was blooming in the river at that time, but weak for dinoflagellates (mainly *Gymnodinium*) ($R^2$ = 0.44). A synthesis of the DMSV and the CASI data indicated that even the existing DMSV bands (centred at 450, 550, 650 and 770 nm) could provide the capability to identify most bloom types in the river system. However, for blooms with spectral characteristics such as *Gymnodinium's,* this relationship would not be expected to be strong.

In the present study the DMSV did not, with its existing band combinations, show any satisfactory relationship with in situ measurements. This suggests that, for blooms like *Gymnodinium*, the system as currently configured could not reliably be used to quantify the bloom concentrations. The lack of characteristic diagnostic features (Figure 16) and the dynamic movement of the bloom over time suggests that, even if clear diagnostic bands were available, it might not be possible to estimate *Gymnodinium* concentrations in the river from the air.

Water clarity and the biology of the particular phytoplankton species may also affect the ability of remote sensing platforms such as DMSV to describe accurately a bloom's distribution and abundance within the water column. This may not be a problem for surface-forming blooms (e.g. cyanobacteria; Jupp et al., 1994) that are easily detectable remotely. However, for microalgae such as *Gymnodinium,* which can change their distribution within the water column, it is essential that remote sensing flights coincide with maximum daily abundance at the water surface if the magnitude and extent of the bloom is to be determined.

In summary, quantifying in-water data on algal blooms with the aid of data from remote sensing requires ground sampling to be done simultaneously — or within minutes — of the remote sensing flight. The flights must coincide with the phytoplankton's daily afternoon migration to the surface waters, and at times of the day that will minimise sunglint. If flights are not so timed, remotely sensed images will not clearly indicate bloom distribution and abundance. A good relationship between the ground data and the images is obviously necessary for detecting and estimating bloom concentrations. However, in situations where blooms are rapidly changing, remote sensing is an effective tool for describing, qualitatively the dynamic nature of the bloom at a particular moment over large spatial scales.

# Recommendations

The findings of our research into the use of remote sensing of the Swan River and surrounding waterways, using airborne systems, identified some of the advantages and limitations to the generic use of this technology. The following points, with the supporting images, illustrate these considerations.

- Remote sensing is an effective means of rapidly mapping the extent of highly dynamic, widely spread algal blooms. Airborne sensors have the advantage over sampling that they can sample large expanses, inexpensively, and quickly. *Remote sensing provides a "birds-eye view" of blooms and provides a unique means of identifying specific sites of interest, such as inflowing drains and "hot-spot" sites, which may be difficult to identify or locate from the ground* (Figure 18).
- Most algal bloom types can be discriminated with a selection of a few spectral bands in the visible spectrum that cover the main combinations of pigments. *For routine monitoring, simple instruments such as the DMSV may be sufficient, provided bandpass filters are selected to provide maximum discrimination of the bloom of interest in the water column.*
- More research on the spectral contribution of water-column components (e.g. humics, suspended solids) could provide a more quantitative description of bloom type and severity through specific algorithms for image analysis.
- A number of factors can result in artefacts in the DMSV images that limit the usefulness of data, hence the need to interpret accurately the extent and severity of a bloom. Some factors can be minimised by careful flight planning and adopting the following protocol:
  - Flight times should coincide with sun angles of < 45 degrees (which usually means that in summer, flights should be between 8 am and 10am, and from 3 pm to 5 pm. *Some algal species such as* Gymnodinium *migrate in the water column, so their highest abundance in the surface layers is in the latter part of the day. Flights need to be planned to coincide with the best physical and biological conditions for maximum accuracy.*
  - A 50% overlap of the DMSV image frames minimises the effects of sunglint. Optimum data quality is obtained when conditions are calm and wave ripples are small. This minimises sunglint and also reduces mixing of the upper water column. The central flight-line for the aircraft can also be set to the same side of the river as the sun to minimise sunglint.
  - Flight altitudes of 3,500 m provide DMSV images with 2 m pixels (nominal ground resolution), which give excellent spatial discrimination.
  - Calibration targets should be included in every mission and gains and offsets of cameras should not be changed without flying again over those targets.
  - Camera alignment on the DMSV should be precise to ensure a minimum of post-processing registration of pixels and easy mosaicing of individual frames when overlain on satellite data such as panchromatic SPOT.

- Further development of automatic correlation-based software procedures to process data for near-real time information products is essential. *Using procedures developed for this study the delivery time for image products is of the order of two to three days. This should be reduced to less than 24 hrs.*
- Ground-truthing must be done within ± 30 min of flight times or bloom distribution and abundance may have significantly changed and have little resemblance to the precise patterns captured in the image. *A way to ensure better ground-truthing at the time of the overflight is to deploy multiple fluorometers from stations or from boats equipped with differential GPS.*

■ The recently developed miniature field spectrometers have the potential to supplement fluorometers and to be useful for remote monitoring and identification of algal types based on characteristic spectra, as well as validating airborne imagery.

# Acknowledgments

The authors thank the following people and their organisations for their contributions: Peter Jolly, and John Parslow of the CSIRO Division of Fisheries; Alex Wyllie and Robert "Red" Shaw of the Remote Sensing Applications Centre (DOLA); Officers of the (then) Waterways Commission (now the Waters and Rivers Commission) and Swan River Trust including Bruce Hamilton, Robert Atkins, Malcolm Robb and the inspectors who operated the *Jack Mattison*; Roger Schultz and Ron Dercoles of the WA Chemistry Centre; Donald DeVries of the CSIRO Office of Space Science and Applications (COSSA ), David Jupp and Richard Davis. Valuable advice in the design of the study, analyses and processing of data was provided by Jeremy Wallace, Suzanne Furby and Peter Thompson. SpecTerra Systems supplied the DMSV. This work received funds and/or research-in-kind from the CSIRO Division of Fisheries, the CSIRO Blue-Green Algal Program, COSSA and the Waters and Rivers Commission of Western Australia. Comments by Ian McLeod and Brian Long improved this report.

# References


Anderson, D. M. (1989). Toxic algal blooms and red tides: A global perspective. In: *Red Tides: Biology, Environmental Science and Toxicology.* T. Okaichi et al., (eds), Elsevier, New York: 11-16.

Babey, S. K. and Anger C. D. (1989). A Compact Airborne Spectrographic Imager (CASI). *Proc. IGARSS 12th Canadian Symposium on Remote Sensing,* Vancouver, BC July 10-14, Vol. 2: 1028-1031.

Campbell, N. A. (1984). Canonical variate analysis - A general model formulation. *Australian Journal of Statistics* **26 (1)**: 86-96.

Campbell, N. A. and Atchely, W. R. (1981). The geometry of canonical variate analysis. *Systematic Zoology* **30 (3)**: 268-280.

Carpenter, D. J. and Carpenter, S. M. (1983). Modelling inland water quality using Landsat data. *Remote Sensing of Environment* **13**: 345.

Dwivedi, R. M. and Narain, A. (1987). Remote sensing of phytoplankton: an attempt from the Landsat Thematic Mapper. *International Journal of Remote Sensing,* **8**:1563.

Harrison, B. A., Jupp, D. L. B. (1991). Introduction to remotely sensed data. *Part 1, microBRIAN Resource Manual.* CSIRO Publications, Melbourne, 141 pp.

Hallegraeff G. M. (1992). Harmful Algal Blooms in the Australian region. *Marine Pollution Bulletin* **25**: 5-8, 186-190.

Hallegraeff, G. M. (1993). A review of harmful algal blooms and their apparent global increase. *Phycologia* **32**: 79-99.

Hick, P., and Jernakoff, P. (1994). Algal bloom research using CASI data in Western Australia. *Proceedings 7th Australasian Conference on Remote Sensing,* Melbourne. Vol. 2: 736-744.

Hick, P. T., Pattiaratchi, C. and Wyllie, A. (1992) A comparison of two Airborne Multispectral Scanners for determination of chlorophyll pigments in riverine, lacustrine and oceanic environments. *Proceedings of 6th Australasian Conference on Remote Sensing,* Wellington, NZ, Vol. 1: 215-224.

Hick, P., Ong, C., Smith, R. C. G., and Honey, F. R. . (1994). Vegetation assessment and monitoring using Airborne Digital Multispectral Videography: implications for geobotanical prospecting and quantitative pre- and post-mining measurement. *Proceedings 19th Environmental Workshop, Aust. Mining Ind. Council,* Karratha, Oct. 9-14, vol. 4: 178-195.

Hosja, W., Deeley, D. (1994). Harmful phytoplankton surveillance in Western Australia. *Waterways Commission Report* **43**, 99 pp.

John, J.(1987). (ed.), Swan River Estuary, Ecology and Management. Curtin University Environmental. Studies Group Report 1: 71-90.

Johnsen G., Samset O., Granskog L., and Sakshaug, E. (1994). In vivo absorption characteristics in 10 classes of bloom-forming phytoplankton: taxonomic characteristics and responses to photoadaption by means of discriminant and HPLC analysis. *Marine Ecology Progress Series* **105**: 149-157.

Johnstone, P. (1994). Algal bloom research in Australia. A report of current status of issues and the development of national research priorities. *Water Resources Management Committee Occasional Paper WRMC 6,* Agriculture and Resource Management Council of Australia and New Zealand Water Forum, 139 pp.

Jupp, D. L. B., Held, A., Byrne, G., Hutton, P. and McDonald, E. (1992) The potential use of airborne scanning for monitoring algal dynamics in Australian inland waters. *COSSA report* **030**, pp. 1-124.

Jupp D. L. B., Kirk, J. T. O. and Harris, G. P. (1994). Detection, identification and mapping of cyanobacteria- Using remote sensing to measure the optical quality of turbid inland waters. *Australian Journal of Marine and Freshwater Research* **45**: 801-828.

Lavery, P., Pattiaratchi, C., Wyllie, A. and Hick P. T. (1992). Water quality monitoring in estuarine waters using the Landsat Thematic Mapper, *Report ED 573 cp,* pp. 1-27.

Lavery P, Pattiaratchi C, Wyllie A. and Hick P. (1993). Water quality monitoring in estuarine waters using the Landsat Thematic Mapper. Remote Sensing of Environment, 46: 268-280.

Lillesand, T. M., Johnson, W. L, Deuell, R. L., Lindstrom, O. M. and Miesner, D. E. (1983). Use of Landsat data to predict the trophic status Minnesota lakes, *Photogrammetric Engineering and Remote Sensing* **49**: 219.

Lyon R.J.P., Honey, F.R. and Hick, P.T. (1994). Second generation airborne digital multispectral video: evaluation of a DMSV for environmental and vegetation assessment. *Proceedings of 1st International Airborne Remote Sensing Conference,* Strasbourg, France, vol. 2: 105-117.

Ong, C., Wyllie, A. and Hick, P. T. (1994). Mapping marine habitats using Geoscan Mk2 Airborne Multispectral Scanner Data. *Paper No.118, Proceedings 7th Australasian Conference on Remote Sensing,* Melbourne vol 1: 698-705.

Pattiaratchi, C. B., Lavery, P. S., Wyllie, A., and Hick, P. T. (1990). Remote sensing of water quality in Cockburn Sound: Development of multi-temporal algorithms. *University of WA Centre for Water Research Report*, WP607CP, 25 pp.

Pattiaratchi, C., Lavery, P., Wyllie, A. and Hick, P. (1992). Multi-date algorithms for predicting surface water quality parameters in estuarine and coastal waters using Landsat TM data. *Proceedings of the Central Symposium "International Space Year"* Munich, Germany, April 1992, pp. 709-714.

Smayda, T. J. (1990). Novel and nuisance phytoplankton blooms in the sea: Evidence for a global epidemic. In: *Toxic Marine Phytoplankton*. E.Granelli et al., (eds.), Elsevier, New York: 29-40.

Verdin, J. P. (1985). Monitoring water quality conditions in a large Western Reservoir with Landsat imagery, *Photogrammetric Engineering and Remote Sensing* **51**: 343.

Zibordi, G., Parmiggiani, F. and Alberotanza, L. (1990). Application of aircraft multispectral scanner data to algae mapping over the Venice Lagoon. *Remote Sensing of the Environment* **34**: 49-54.

# CSIRO Marine Laboratories

## Division of Fisheries
## Division of Oceanography

Headquarters
Castray Esplanade, Hobart, Tasmania
GPO Box 1538, Hobart, Tasmania 7001, Australia

Queensland Laboratory
133 Middle Street, Cleveland, Queensland 4163

Western Australia Laboratory
Leach Street, Marmion, WA
PO Box 20, North Beach, WA 6020




ISBN 0 643 05792 7
ISSN 0725—4598